Characterization of xyloglucan-specific fucosyltransferase activity in Golgi-enriched microsomal preparations from wheat seedlings

Richard E. Wiemels[1], Wei Zeng[1,2,#], Nan Jiang[1,2$], and Ahmed Faik[1,2*]

[1]Department of Environmental and Plant Biology and [2]Molecular and Cellular Biology Program, Ohio University, Athens, OH 45701, USA

[#]Current address: State Key Laboratory of Subtropical Silviculture, School of Forestry and Biotechnology, Zhejiang A&F University, 666 Wusu St, Lin'an, Zhejiang Provence, Hangzhou, China 311300

[$]Current address: Department of Biochemistry and Molecular Biology, Michigan State University, East Lansing, MI 48823, USA

*Corresponding author: Ahmed Faik

E-mail: faik@ohio.edu

Abstract

Xyloglucan (XyG) is a major hemicellulosic polymer in primary cell walls of dicotyledonous plants but represents only a minor constituent of cell walls from graminaceous monocotyledons (*Poaceae*). Our current information on XyG biosynthesis *in vitro* comes exclusively from studies on dicotyledonous plants. While XyG has been reported in grass cell walls, there are no studies of XyG biosynthesis *in vitro* in grasses. In this report, we investigated XyG structure and biosynthesis in etiolated wheat seedlings and showed that their walls contain small amounts (4-14%) of XyG. Furthermore, structural analysis using electrospray ionization mass spectrometry (ESI-MS) and high pH anion exchange chromatography (HPAEC) revealed that wheat XyG may be of XXGGG-type. Interestingly, detergent extracts from root microsomes were able to fucosylate tamarind XyG *in vitro* in a similar way as fucosyltransferase activity from *Arabidopsis thaliana* (AtFUT1) and pea (PsFUT1). Endoglucanase digestion of the [^{14}C]fucosylated-tamarind XyG formed by the wheat fucosyltransferase activity released radiolabeled oligosaccharides that co-eluted with authentic fucoslyated XyG oligosaccharides (XXFG and XLFG). Although wheat fucosyltransferase activity was low, it appeared to be specific to XyG and required divalent ions (Mg^{2+} or Mn^{2+}) for full activity. Together, these results suggest that the XyG fucosylation mechanism is conserved between monocots and dicots.

Introduction

The hemicellulosic polymer, xyloglucan (XyG), makes up to 35% of the dry weight of primary cell walls of dicotyledonous plants [1-4]. Cell walls from graminaceous monocotyledons (*Poaceae*) contain only 4-10% XyG, and this XyG is structurally less complex than XyG from dicots [2;5;6]. All XyGs consist of a backbone of β-(1,4)-linked glucosyl (Glc) residues, and depending on the substitution pattern of this backbone with α (1,6)-linked xylosyl (Xyl) residues, XyG structure was initially classified into two types, namely XXXG- and XXGG-type [7], where X and G designate substituted and unsubstituted Glc residues in the backbone, respectively (for nomenclature see [8;9]). Other XyG types, such as the XXX-type, have been identified in the coats of *Helipterum eximium* seeds [10], the XXGGG-type in species of the subclass Asteridae [11], and the XXXXG-type in cotyledons of *Hymenaea courbaril* [12]. Based on analytical data from XyG purified from immature barley plants [13] and rice seedlings [14], XXGGG-type was proposed for XyG from grasses with glucan backbone regions having more or less substitution [6;14]. However, the presence and purification of the XXGGG repeating unit itself was not demonstrated.

Side-chain substitutions on XyG have been shown to be structurally diverse and species/tissues/development-dependent. Although it was suggested that Xyl residues of XyG from grasses may occasionally bear terminal galactose (Gal) or arabinofuranose (Ara*f*) residues [6;15;16], this was never experimentally confirmed through purification of the polymer. XyG from Solanaceae is of XXGG-type, and it has been shown that it can be further arabinosylated and/or galactosylated [17]. Several works demonstrated that cell walls of monocots contain fucosylated XyGs [18-20]. In some species, the backbone glucosyl residue can be *O*-acetylated [11;17;21]. The non-xylosylated glucosyl backbone residues of the XXGG-type oligosaccharides

62 are often *O*-acetylated [17], which is not reported in XXXG-type XyGs [22]. According to recent
63 structural studies at least 24 unique, naturally occurring xyloglucan side-chain structures exist
64 [9;22;23]. However, linking this structural diversity of XyG substitutions to physiological
65 functions is still elusive. The Arabidopsis *xlt2 mur3.1* double mutant, in which XyG is lacking
66 galactosyl, fucosyl, and acetyl residues showed a dwarfed plant [24;25].

67 Until now, the biochemistry of XyG biosynthesis *in vitro* has been investigated exclusively in
68 dicots. For example, biochemical studies using microsomal membranes from dicotyledonous
69 plants showed that the incorporation of Glc and Xyl residues into the "xylosyl-glucose"
70 backbone occurs simultaneously, which requires a synergistic/cooperative mechanism between
71 XyG-glucan synthase (XGSase) and XyG-xylosyltransferase (XXT) activities [26-29]. This
72 mechanism has not been confirmed yet in any membrane preparation from monocotyledonous
73 plants. Many Arabidopsis (*Arabidopsis thaliana*) glycosyltransferase (GT) genes involved in
74 XyG biosynthesis have been identified and characterized, providing target genes with which to
75 investigate XyG biosynthesis in other plant species including economically important plants such
76 as wheat, rice, and maize. These genes include a *XyG-fucosyltransferase* (*AtFUT1/MUR2*) from
77 the CAZy GT37 family [30], several *XyG-xylosyltransferases* (*XXTs*) from the GT34 family [31-
78 35], and two *XyG-galactosyltransferases* (*MUR3* and *XLT2*) from the GT47 family [24;36].
79 MUR3 and XLT2 are the galactosyltransferases for addition of Gal to the first and second Xyl
80 residues, respectively, from the reducing of an XXXG unit. The β-(1,4) glucan backbone is
81 synthesized by a XGSase that belongs to cellulose synthase-like C (CSL-C) family [37].

82 One of the major differences between XyGs from dicots and grasses is fucose (Fuc) content.
83 Although there is evidence that fucosylate XyG is present in monocots [6;14;18;19;38;39], and a
84 fucosyltransferase gene has been identified in rice (*Oryza sativa*) genome (using functional

complementation approach [20]), biochemical characterization of fucosyltransferase activity from any plant tissues of the *Poaceae* is lacking. Here, we present evidence of fucosyltransferase activity in microsomal preparation from etiolated wheat seedlings. Interestingly, detergent-solubilized activity from microsomal membranes of root tissues is able to fucosylate tamarind XyG *in vitro* in a similar way as Arabidopsis AtFUT1 and Pea PsFUT1 enzymes. Structural analysis of XyG oligosaccharides (XyGOs), released by treatment with a XyG-specific endoglucanase, suggested that cell walls of wheat roots may contain XyG of two types: XXGGG- and XXXG-type. Although we show that these XyG types contain Fuc, Gal, and Ara residues, we were not able to determine whether they constitute different domains of the same polymer or are part of two distinct polymers synthesized by different machineries. To our knowledge this work represents the first report on the biochemical characterization of a XyG fucosyltransferase activity in grasses, and thereby furthers our understanding of XyG biosynthesis in monocots.

Results

Xyloglucan from etiolated wheat seedling walls contains Fuc, Gal, and Ara residues

We reasoned that if XyG from wheat seedlings are fucosylated, we should be able to detect the presence of oligosaccharides containing Fuc and Gal in KOH extracts of wheat cell walls. Thus, alcohol insoluble residues (AIR) prepared from cell walls of 6-day old etiolated wheat seedlings were directly treated with 4M KOH to extract the non-cellulosic polymers, and XyGOs were released by enzymatic treatment of these extracts with a purified XyG-specific endoglucanase (XG5, [40]). Typically, 4M KOH solubilized ~25% and ~33% (w/w, based on phenol-sulfuric assay) of the wall material from roots and shoots, respectively. Treatment of these alkali extracts with XG5 released ~13% and ~46% (w/w, based on phenol-sulfuric assay) of the material, respectively. Control reactions containing boiled XG5 enzyme released less than 0.5% of the material. These results allowed us to roughly estimate XyG contents in wheat root and shoot to ~4 and ~14% (w/w), respectively.

Next, the endoglucanase-released material was analyzed for monosaccharide composition through total acid hydrolysis followed by HPAEC fractionation. Purified XyG from pea treated in the same conditions and same enzyme was used as a positive control. As expected, Glc and Xyl were the two main monosaccharides in all XyGOs (pea and wheat) and Gal, Ara, and Fuc were also present, but at lower amounts (Table 1). According to our estimates, Gal and Fuc contents represent 5 mol% and <0.5 mol% in root oligosaccharide mixtures, respectively (Table 1), suggesting that only a small fraction of the Gal is fucosylated. The identity of Fuc from wheat XyGOs was further confirmed using gas chromatography-mass spectrometry (GC-MS) analysis (data not shown). The Glc:Xyl ratio in wheat XyG from roots and shoots is 2.19 and 2.27, respectively; compared to a mixture of pea XyG oligosaccharides (released with XG5 treatment)

from which has a Glc:Xyl ratio of 1.22 (Table 1). As a control, analysis of pea XyGOs generated the expected ratios Glc:Xyl:Gal:Fuc of 7.5:6:1.7:1, respectively, which are typical of primary wall XyGs from dicots [1;41]. However, despite purification, XG5 endoglucanase was still contaminated with β-glucan hydrolase activity (lichenase, see below), which can act on β(1,3)(1,4)-mixed-linkage glucan (MLG, an abundant polymer in cell walls of grasses) that explain the overestimated Glc amount in wheat XyGOs. In conclusion, monosaccharide analysis suggests the presence of Fuc in XyGOs from wheat root but not detectable in XyGOs from shoots. Also, the detection of Ara in this analysis would suggest the presence of an arabinosylated side chain in wheat XyG.

We next analyzed wheat XyGOs by electrospray ionization mass spectrometry (ESI-MS) and ESI-MS/MS. As indicated in Figure 1, the XG5-released XyGOs showed signal ions that are characteristic of XyGs, namely ions at mass/charge ratio *m/z* 792, *m/z* 953, *m/z* 1085, *m/z* 1115, and *m/z* 1247 (all as sodiated ions $[M+Na]^+$) corresponding to oligosaccharides having 3 hexoses (Hex) and 2 pentoses (Hex3Pen2), Hex4Pen2, Hex4Pen3, Hex5Pen2, and Hex5Pen3, respectively. Importantly, all the ions detected were absent in control reactions where boiled XG5 enzyme was used (Fig. 1C). Purified XyGOs from etiolated pea seedlings were included as a positive control and, as expected, the most abundant oligosaccharides were XXXG, XLXG/XXLG, and XXFG corresponding to ions at *m/z* 1085, 1247, and 1393 (all as $[M+Na]^+$), respectively (Fig. 1D). The ions at *m/z* 792 (Hex3Pen2), *m/z* 953 (Hex4Pen2), and *m/z* 1115 (Hex5Pen2), which were observed in wheat XyGOs but not in pea XyGOs, suggest that at least a part of the glucan backbone of wheat XyGs is less substituted with Xyl residues. On the other hand, the ions at *m/z* 1085 (Hex4Pen3) and *m/z* 1247 (Hex5Pen3), which were present in both wheat and pea XyGOs, may indicate that some regions of the backbone may contain “Gal-Xyl”

(L) and/or "Ara-Xyl" (S) side chains (Fig. 1). We also consistently observed ions at *m/z* 1013 and 1175 that correspond to oligosaccharides having six hexoses (Hex6) and seven hexoses (Hex7), respectively, supporting the presence of MLG oligosaccharides due to lichenase activity contamination in our XG5 preparation, despite our efforts to purify XG5 activity from the original enzyme preparation. This was further confirmed by testing our purified XG5 preparation on MLG from barely, which released gluco-oligosaccharides including Hex6 and Hex7 oligosaccharides (data not shown).

To gain more insights about the structures of the wheat XyGOs, their fragmentation patterns was analyzed by collision-induced dissociation (CID)-MS/MS). CID-MS/MS fragmentation induces the cleavage of both glycosidic bonds and bonds within the sugar ring [42;43]. The cleavage of glycosidic bonds usually results in the loss of either the whole sugar molecule (e.g. 180Da for Glc) from the reducing end, or the sugar molecule minus water (e.g. 162Da for Glc) from the non-reducing end [42]. However, cleavage of a sugar ring yields so-called cross-ring fragments as a result of a loss of the acidic residue ($^{k,l}A_n$ ions, see [42] for nomenclature). Furthermore, XG5 endoglucanase only cleaves XyG backbone between an unbranched and a branched Glc residues [40]. Based on this mode of action, the end products of XG5 should be XyGOs with one or more unbranched Glc residues at their reducing ends and no unbranched Glc residues at their non-reducing ends. CID-MS/MS fragmentation analysis of the ion at *m/z* 792 (Hex3Pen2, $[M+Na]^+$) depicted in Figure 2A showed the presence of four abundant product ions formed by loss of 18, 60, 120, and 132Da from the parent ion. Loss of 60 and 120Da were the result of cross-ring fragmentation of the Glc residue at the reducing end, indicating that most Hex3Pen2 oligosaccharides have at least one unbranched Glc at their reducing ends. Loss of 132Da (Xyl minus water molecule) resulted in the production of the ion at *m/z* 659 (Fig. 2A).

168 This fragmentation pattern supports the presence of XXG fragments among the Hex3Pen2
169 oligosaccharides. Similarly, CID-MS/MS analysis of the ion at *m/z* 953 (Hex4Pen2, $[M+Na]^+$)
170 resulted in cross-ring fragmentation of the Glc residue at the reducing end, as indicated by the
171 three abundant ion signals corresponding to the loss of 18, 60, and 120Da from the parent ion
172 (Fig. 2B). The ion signals at *m/z* 644 and 660, which are the result of the loss of a disaccharide
173 "Hex-Pen" from the non-reducing end, and the ion at *m/z* 791 are due to the loss of a
174 disaccharide "Hex-Hex" from the reducing end. Based on the mode of action of XG5 and the
175 fragmentation pattern of the parent ion, XXGG is the most abundant oligosaccharide in the
176 Hex4Pen2 XyGO mixture. Furthermore, the ion signals at *m/z* 701, 731, and 761 resulting from
177 cross-ring fragmentation of the second Glc residue at the reducing end provide additional support
178 to the presence of two Glc residues at the reducing end (Fig. 2B).

179 Fragmentation of the ion at *m/z* 1085 (Hex4Pen3, $[M+Na]^+$) also resulted in cross-ring
180 fragmentation ions at the Glc residue of the reducing end (*m/z* 1067, 1025, and 965, Fig. 1C).
181 While the ion signals at *m/z* 773 and 791 are due to a loss of a "Xyl-Glc" disaccharide from the
182 non-reducing end, the ions at *m/z* 905 and 923 correspond to the loss of two Hex residues (i.e.,
183 "Glc-Glc" disaccharide) from the reducing end. Importantly, the presence of the ion at *m/z* 821,
184 which can be formed only if two pentoses are lost at the same time (Fig. 1C), is an indication of
185 XyGOs may have "Xyl-Xyl" (U) and/or "Ara-Xyl" (S) side chains. Therefore, the most likely
186 structure of this oligosaccharide is XSGG (Fig. 2C).

187 Fragmentation of the ion *m/z* 1115 ($[M+Na]^+$) representing Hex5Pen2 oligosaccharides
188 showed a more complex spectrum, suggesting a mixture of XyGO structures such as XXGGG,
189 XLGG/LXGG, and SGGGG. Most of the ion signals are due to cross-ring fragmentation of two
190 or three unbranched Glc at the reducing end (Fig. 2D). The loss of the trisaccharide "Gal-Xyl-

Glc" from the non-reducing end resulted in the formation of a weaker ion signal at *m/z* 641 and supports the presence of an LXGG structure (Fig. 2D). Similarly, the ion signal at *m/z* 851, corresponding to an oligosaccharide containing five Hex residues is a result of the loss of "Ara-Xyl" disaccharide (S side-chain) from the non-reducing end of SGGGG (Fig. 2D). The presence of this oligosaccharide is also supported by the ion signals at *m/z* 671 and 687, which are due to the loss of "Ara-Xyl-Glc" trisaccharide from its non-reducing end (Fig. 2D).

CID-MS/MS spectrum of the ion *m/z* 1247 (Hex5Pen3, $[M+Na]^+$) also showed a complex spectrum (data not shown) that was difficult to interpret. However, careful analysis of this spectrum suggested a mixture of XyGOs having structures similar to *m/z* 1115 with an additional pentose (most likely Xyl) forming the following possible XyGO structures: SXGGG/XSGGG, XXXGG, XLXG/XXLG, and SLGG. This means either that XyG from wheat roots has XXXG and XLXG/XXLG structures (found in dicot plants) or these tissues produce a polymer that has both 4-unit backbone repeats and 5-unit backbone repeats. Because of the low content of Fuc in wheat XyG, we were not able to identify fucosylated XyGOs or purify oligosaccharides containing Fuc and/or Gal. Further work is required to determine the fine structure of wheat XyG(s). Only when successful purification of wheat XyG polymer is achieved can the fine structure be determined.

Microsomal fractions from roots but not shoots of etiolated wheat seedlings contain XyG-fucosyltransferase activity with similar biochemical characteristics as AtFUT1 and PsFUT1 activity

The presence of fucosylated XyG in cell walls of etiolated wheat seedlings suggests that a XyG-specific fucosyltransferase activity is present in these tissues. To investigate this hypothesis,

Triton X100-solubilized proteins from Golgi-enriched microsomes from etiolated wheat seedlings (coleoptile and root) were tested for their ability to transfer [^{14}C]Fuc from GDP-[^{14}C]Fuc onto tamarind XyG in a standard XyG fucosyltransferase assay [44]. As indicated in Table 2, substantial fucosyltransferase activity was observed in wheat root tissues, which is in agreement with the fact that Fuc was detected in XyGOs from cell walls of wheat seedling root. However, the wheat XyG-fucosyltransferase specific activity (~30 pmol Fuc incorporated per hour per mg protein) was ~10-times less than was detected in equivalent detergent solubilized extracts from pea microsomes used as a positive control (Table 2). This activity was only detected in roots, as Triton X-100 extracts from wheat coleoptiles (shoots) did not transfer any radioactivity onto tamarind XyG (Table 2). Time course analysis of wheat XyG-fucosyltransferase activity from detergent extracts of microsomes prepared from roots harvested at various developmental stages, namely five, eight, and 11 days after germination, indicated that tissues from 5-day old wheat seedlings have the highest XyG-fucosyltransferase activity (Fig. 3A), suggesting that the activity is developmentally regulated. This is consistent with results from studies of XyG-fucosyltransferase activities in pea and Arabidopsis where higher activities were observed in young and rapidly dividing tissues [30;36]. XyG-fucosyltransferase activity was also detected in the roots of etiolated Brachypodium seedlings, though the activity was 10 times lower than in wheat (data not shown). Furthermore, wheat fucosyltransferase activity is specific for XyG, as other cell wall polymers such as rhamnogalacturonan-I (RG-I), known to contain terminal α-fucosyl residues, [45], arabinan, and pectic galactan were not good acceptor substrate in the assay (Fig. 3C).

In a second experiment, we investigated the metal ion dependence of wheat XyG-fucosyltransferase activity in the presence and absence of various divalent cations. Wheat XyG-

fucosyltransferase activity does not require divalent cations for activity; however, the addition of 5mM $MgCl_2$ more than doubled activity, and addition of $CaCl_2$ enhanced activity by ~40% and $MnCl_2$ had no effect (Fig. 4A), which is consistent with the previous study on XyG-fucosyltransferase activity in pea [29]. Wheat XyG-fucosyltransferase activity is optimal at ~pH 6 (Fig. 4B), which is also consistent with pea XyG-fucosyltransferase activity [29]. Finally, wheat activity is specific for GDP-Fuc because GDP-mannose and GDP-Glc did not produce any product with tamarind XyG (data not shown).

Wheat enzyme activity fucosylates tamarind XyG in a similar way as pea enzyme activity

Next, we wanted to verify whether wheat XyG-fucosyltransferase activity fucosylates tamarind XyG in a similar manner as the activity from pea [29]. Thus, the product "[^{14}C]Fuc-tamarind XyG" generated by the wheat microsomal extracts was treated with an endoglucanase (E-CELTR, Megazyme) and the released [^{14}C]radiolabeled fragments were fractionated by high pH anion exchange chromatography (HPAEC). Figure 4C shows a typical elution profile of these fragments and indicates that over 50% of the [^{14}C]radiolabel co-eluted with two authentic fucosylated XyGOs, XXFG and XLFG, generated and purified from pea XyG. Around 25% of the [^{14}C]radiolabel eluted at ~4min and may be attributed to free [^{14}C]Fuc. Around 18% of the [^{14}C]radiolabel eluted as smaller XyGOs with unknown structure at around eight minutes (Fig. 4C). However, previous work showed that XFG, LFG, and FG usually elute in this time range on CarboPac-PA-100 column [46]. The [^{14}C]products from a control reaction (lacking tamarind XyG) were digested and analyzed under the same conditions. As indicated in Figure 4C, the three main peaks (XXFG, XLFG, and unknown XyGOs) were absent, and the peak at 2-3min was present. These data support the conclusion that the detergent-solubilized wheat activity from

microsomal membranes of etiolated wheat have a XyG-dependent fucosyltransferase activity that can fucosylate tamarind XyG to generate a polymer that contains XXFG and XLFG oligosaccharides. In addition, we found that the incorporation of [^{14}C]Fuc was greater with tamarind XyG as an acceptor compared to XyG from nasturtium seed (data not shown), which might be explained by the difference in the fine structure of these two storage XyGs. Tamarind XyG has relatively more XXLG subunits compared to nasturtium XyG [47]; XXLG was shown to be a better acceptor for the fucosyltransfer reaction in pea [29]. There was no sign of products fucosylated closer to the non-reducing end of the subunits, e.g. XFXG or XFLG. We would expect these subunits to elute differently from one another but closer to XXFG and XLFG. No peak corresponding to labeled XFFG was observed, which would elute from this column at a different locus from XXFG and XLFG, as it does after HPLC on a Dynamax-60A NH_2 column [48]. Thus, we conclude that wheat XyG-fucosyltransferase activity is specific for fucosylation of galactosyl residues nearest the reducing end of XyG subunits.

Identification of wheat members of the GT37 family

To gain further insights into fucosylation of XyG in wheat seedlings, we sought to identify putative wheat fucosyltransferases (FUTs) in public genomics resources (Table 3). As of June 2019, CAZy database lists only one wheat member (CAMPLR22A2D_LOCUS5750). Using bioinformatics approach (see Materials and Methods for detailed approach), we identified 16 wheat members of the GT37 family (not including homeologs), a number that is comparable to rice whose genome contains 17 GT37 members. These wheat FUTs were named TaFUT-A through TaFUT-P (Table 4). Of the 16 wheat members, only four were full-length (*TaFUT-A*, *TaFUT-B*, *TaFUT-C*, and *TaFUT-H*), and three wheat genes (*TaFUT-D*, *TaFUT-F*, and *TaFUT-*

283 *O*, Table 4) were cloned in this study. To facilitate the identification of wheat genes that cluster
284 with the two known XyG-fucosyltransferases at the time of performing this work: AtFUT1 and
285 PsFUT1 (from pea, *Pisum sativum* L.), we carried out phylogenetic analysis using Arabidopsis,
286 rice and wheat members of the GT37 family. According to phylogenetic analysis, wheat
287 orthologs of all rice genes were identified, except for Os08g0334900 (Fig. 5A). Rice and wheat
288 FUTs clustered into two major groups (II and III) and a smaller group (group IV). Group II and
289 III can be further split into two subgroups (A and B) that cluster in the same branch as FUTs
290 from dicots (Fig. 5A). Phylogenetic analysis also showed that FUTs from dicots (Arabidopsis
291 and Pea) clustered together in a clade (group I) that contains no rice or wheat FUTs (Fig. 5A).
292 Thus, the phylogenetic analysis could not resolve the relationship between the known XyG-
293 fucosyltransferases (AtFUT1 and PsFUT1) and putative rice and wheat FUTs. Even pairing of
294 AtFUT1 and PsFUT1 (both are from two dicot species) was not possible (Fig. 5A). It seems that
295 the FUTs have independently diverged in each plant lineage, which makes identification of grass
296 orthologs of characterized FUTs not possible using phylogeny. Although, group IV (TaFUT-O
297 and Os02g0764400) are phylogenetically the most closely related to AtUT1 and PsFUT1 (Fig.
298 5A), pairwise alignments of the full-length putative grass FUTs in groups II-A and II-B (8
299 putative wheat FUTs) with Arabidopsis FUTs (group I) showed high sequence identity/similarity
300 with AtFUT1 and PsFUT1 compared to any other Arabidopsis FUT sequence. This makes the
301 selection of wheat candidates for testing even more challenging. TaFUT-O showed 54% identity
302 at the amino acid level (67-69% similarity) with PsFUT1 and AtFUT1. Thus, *TaFUT-O* was
303 chosen for enzyme assay testing. We also selected arbitrary TaFUT-F and TaFUT-D from group
304 II-B.

Since XyG-fucosyltransferase activity is detected in roots, we reasoned that its encoding gene must be highly expressed in roots compared to shoots. Thus, in a second step, we sought to determine the levels of expression of wheat FUT genes in roots and shoots using RT-PCR technique. For this experiment, we focused on 8 wheat FUT genes (*TaFUT-A*, *TaFUT-B*, *TaFUT-C*, *TaFUT-D*, *TaFUT-E*, *TaFUT-F*, *TaFUT-G*, *TaFUT-I*, and *TaFUT-O*), since they were either full-length or have enough long nucleic sequence to design gene-specific primers. Our RT-PCR results summarized in Figure 5B shows that *TaFUT-A*, *TaFUT-B*, *TaFUT-D*, and *TaFUT-O* are expressed in roots and shoots at almost equal levels, while *TaFUT-F* and *TaFUT-I* are expressed predominantly in roots (with TaFUT-I having very low expression level). *TaFUT-C* transcript was not detectable in both roots and shoots (Fig. 5B). Thus, according to expression data, either or both TaFUT-F and TaFUT-I could be XyG-fucosyltransferases. By the time this work was completed, a rice XyG-fucosyltransferase gene (*Os02g0764400*) was identified through complementation of Arabidopsis *axy2.2* mutant [20]. While Os02g0764400, TaFUT-F, and TaFUT-I clustered together in group II-B, TaFUT-I is the closest homolog to Os02g0764400 (both located in the same branch, Fig. 5A). At the time of performing this work, TaFUT-I (Traes_6DL_B04B4C48D.1, Table 3) was not among the 13 wheat FUT sequences publicly available. It was identified after the recent early release of species in Phytozome v12.1.6. In addition, expression data indicate that *TaFUT-I* has very low expression levels in roots. Therefore, we did not include TaFUT-I in our original work and focused on TaFUT-F and TaFUT-O for enzyme activity testing.

His-tagged versions of TaFUT-F and TaFUT-O were produced in Pichia cells and detergent-solubilized proteins were prepared from independent transgenic yeast cell lines, each expressing one of these putative FUT genes. Expression of these putative FUTs was confirmed by western

328 blot analysis using the 6xHis antibody. Detergent-solubilized proteins from microsomal
329 membranes were used in the FUT assay as described in [44]. Unfortunately, none of the
330 detergent extracts showed XyG-dependent activity (data not shown). More work is needed to
331 identify wheat XyG-fucosyltransferase gene.
332

Discussion

Etiolated seedlings have been studied extensively in many plants, including cereals, as they represent relatively simple and homogenous tissues with active primary cell wall metabolism. The growth of the shoots (coleoptiles) in these etiolated seedlings occurs mainly through rapid and intensive elongation of cells and cell wall material synthesis [6;49;50]. Thus, etiolated seedlings are a good model to investigate polysaccharide biosynthesis in primary cell walls. Using this plant system, we showed that detergent-solubilized extracts from Golgi-enriched microsomal membranes from roots were able to fucosylate tamarind XyG *in vitro*. This activity was higher in younger seedlings when elongation of cells and cell wall synthesis are at their maxima. This finding has an important implication as it indicates that wheat XyG contains some "L" side chains because a XyG-fucosyltransferase activity *in vivo* in wheat can only be expected if the galactosylated accepter contains "L" side chains (*i.e.*, XXLG, XLGG, or possibly XLGGG). However, such a galactosylated substrate has never been unambiguously and directly demonstrated in XyG from *Poaceae*. Based on linkage data, Sims et al. [16] suggested that side chains in XyGs from *Poaceae* might contain Gal and Ara residues. However, the authors conceded that further studies would be necessary to confirm such structures. Our data is in agreement with previous work showing evidence that monocots cell walls contain fucosylate XyG [6;14;18;19;39;40;51]. Using ESI-MS analysis of XyGOs released from AIR preparation by treatment with purified XyG-specific endoglucanase, XG5 [40], we showed that XyG contents in wheat root and coleoptile (shoots) walls were roughly estimated at ~4 and ~14%, respectively. These levels are comparable to published data in other cereals such as barley seedlings [6;52;53] suspension-cultured maize cells [54], rice endosperm [55], and rice seedlings [14]. The observed difference in XyG content between coleoptile and root walls may be

356 explained by a difference in XyG biosynthesis and turnover, which are usually associated with
357 rapid cell expansion in dicots, and a similar observation was also reported for some
358 graminaceous monocots [56]. In the case of etiolated wheat seedlings, shoot cells undertake
359 extensive and rapid expansion (compared to root) during growth, which may explain their 3.5-
360 times more XyG content compared to root walls. Although the walls of wheat shoots contain
361 more XyG compared to root walls, XyG-fucosylatransferase activity was mostly confined to
362 roots. Recent analysis of XyGs in rice showed that fucosylated XyG is also confined to young
363 root tissues [20]. The presence of fucosylated XyG in other grasses, such as miscanthus, foxtail
364 millet, and rice, was indirectly demonstrated using specific antibodies for fucosylated XyG (i.e.,
365 CCRC-M1 and CCRC-M106) [57]. Further analysis of wheat shoot XyGOs released by XG5
366 treatment using CID-MS/MS revealed the presence of oligosaccharides that can only be
367 attributed to a XyG of the XXGGG-type. These XyGOs seem to come from XyG domains of
368 limited or no substitution (e.g. XXGGG and SGGGG) and domains with greater substitution
369 (e.g. XXXG and XLGG) that contain “L” side chain. The presence of an ion at *m/z* 1247
370 (Hex5Pen3, Fig. 1) in XyGOs from root tissues of wheat may suggest the presence of XyG of
371 XXXG-type in these tissues. This ion was absent in XyGOs from wheat shoots. Although we
372 were not able to identify unambiguously the presence of XXFG or XXLG structures
373 characteristic of XyG of XXXG-type, our data is in agreement with a recent study showing that
374 cell walls of young root tissues in rice contain XyG of XXXG-type, but not in shoot tissues [20].
375 Unfortunately, our ESI-MS instrument is not sensitive enough to detect low amounts of
376 fucosylated XyGOs, however monosaccharide analysis and GC-MS strongly support the
377 presence of Fuc, Gal, and Ara in XyGOs from wheat roots (data not shown).

To further confirm the presence of fucosylated XyG in wheat, we sought to determine whether wheat roots contain a XyG-fucosyltransferase activity responsible for the incorporation of Fuc into XyG in their tissues. Our data indicate that detergent-solubilized proteins from root tissues have the capacity to transfer radiolabeled [^{14}C]Fuc from GDP-[^{14}C]Fuc onto tamarind XyG *in vitro*. Shoot tissues did not show any detectable activity. This result was expected, as fucosylated XyG was detected in roots and not in shoots (under our conditions). It is possible that shoots may have "F" side chain, but their amounts must be below detection limit for our instrument. A recent work in rice identified a XyG-fucosyltransferase gene (*Os02g0764200, OsMUR2*) through functional complementation approach [20]. However, the rice XyG-fucosyltransferase activity has not been characterized biochemically. Wheat XyG-fucosyltransferase described here shares biochemical characteristics with activity from pea including no requirement for divalent cations, enhancement of activity with addition of $MgCl_2$ and $CaCl_2$ and no enhancement of activity with the addition of $MnCl_2$ [29]. These similar biochemical attributes suggest that these activities are the same and that the wheat XyG-fucosyltransferase is encoded by a member of the same GT family (GT37 family in the CAZy database, which is a plant-specific GT family [58]). GT37 family also includes two Arabidopsis α(1,2)fucosyltransferases specific for arabinogalactan-proteins (AGPs), AtFUT4 and AtFUT6 [59]. In Arabidopsis, a single gene, *AtFUT1*, is responsible for XyG fucosylation, as the *mur2* mutant that has a lesion in the *AtFUT1* gene completely lacks fucosylated XyG [60]. Currently, there is no genetic evidence to demonstrate that *OsMUR2* is a single gene responsible for XyG fucosylation in rice. According to eFP platform (http://bar.utoronto.ca/efprice/cgi-bin/efpWeb.cgi), the expression of *Os06g0212100* is also confined to roots in rice, similar to

400 *OsMUR2* (Fig. 6), which may suggest more than one XyG-FUT genes exist in rice. The ortholog
401 of *Os06g0212100* in wheat (*TaFUT-G*) has very low expression levels in roots (Fig. 5B).
402 Despite the identification of wheat XyG-fucosyltransferase activity, phylogenetic and
403 expression profile analyses were not sufficient to identify true wheat orthologous proteins to
404 AtFUT1 and PsFUT1. By the time this work was completed, the rice XyG-fucosyltransferase
405 (Os02g0764200, OsMUR2) was not identified yet. At that time the wheat gene encoding for
406 TaFUT-O was the most logical and promising candidate, as it is phylogenetically the most
407 closely related to AtFUT1 and PsFUT1 (located in the same branch, Fig. 5A). However, *TaFUT-*
408 *O* is expressed in both roots and shoots at similar levels, which does not fit with the fact that
409 fucosylated XyG was mostly detected in roots and no detectable activity could be measured in
410 shoots. According to expression data, the next most promising candidates are *TaFUT-F* and
411 *TaFUT-I*, as they were expressed more highly in wheat roots than in shoots (Fig. 5B). Since we
412 did not identify *TaFUT-I* through our strategy (sequence quality was low and was eliminated),
413 we focused on *TaFUT-F*, as a second potential candidate. Unfortunately, none of these wheat
414 FUTs showed *in vitro* XyG transfer activity. The recent early release of species at Phytozome 12
415 allowed the identification of *TaFUT-I*, which is the ortholog gene of *OsMUR2* in wheat. The
416 failure of phylogenetic analysis in identifying the genuine wheat ortholog of AtFUT1 and
417 PsFUT1 underscores the limitations of bioinformatics approach in identifying orthologs in
418 protein families having a high degree of homology, such as the GT37 family. FUTs within a
419 given plant tend to cluster more closely with each other than with FUTs from other plants. Thus,
420 the only ways to identify functional orthologs is by heterologous expression/activity assays or by
421 mutant complementation. It is challenging to select promising wheat candidates for functional
422 analysis based only on amino acid sequence similarity to AtFUT1 and PsFUT1. For example,

Os02g0764400 was previously identified as the only AtFUT1 ortholog in rice based on amino acid sequence similarity [61]. Overexpression of *Os02g0764400* in Arabidopsis *axy2.2* mutant did not restore XyG fucosylation. TaFUT-O is the closest homolog to Os02g0764400 in wheat (Fig. 5A), and our results also showed that TaFUT-O lacks XyG-fucosyltransferase activity, which is consistent with genetic complementation data from *Os02g0764400*.

The presence of Fuc residues in root XyG and less in coleoptile XyG is puzzling. One possible explanation could be the physiological role of Fuc residues in root interactions with microorganisms in soil. Several plant pathogens such as *Ralstonia solanacearum* and *Pseudomonas aeruginosa* produce L-Fuc-binding lectins. Interestingly, the lectin from *Ralstonia solanacearum* showed a strong affinity toward fucosylated XyG of XXXG-type [62]. Knockdown of the *PsFUT1* transcript in pea roots results in a phenotype of wrinkled and collapsed cells visible through SEM [63]. In grasses, a Fuc deficient mutant or XyG-fucosylatranferase gene knockout is not available for comparison, and it is unknown if grasses conserved the ability to substitute Fuc with L-Gal. The possible explanation of non-detection of fucosylation of XyG in wheat coleoptile using our ESI-MS instrument could be that it occurs at specific developmental stages and Fuc is removed by a fucosidase activity in later developmental stages. We showed that XyG-fucosyltransferase activity was higher in 5-day old seedlings and decreased drastically at 8 days of growth. No attempts were made to analyze XyG from roots of 8-day old wheat seedling to determine whether fucosylation of XyG occured at early developmental stages is maintained in walls of older seedling. Tissue-specific differences in XyG fucosylation are not unusual in plants. For example, certain species within the *Poaceae* appear to have phloem cells containing fucosylated XyG, while neighboring cells do not [18].

Also in the *Solanaceae*, fucosylated XyG of XXXG-type has been observed specifically in pollen tubes [64].

In conclusion, our present work demonstrates that etiolated wheat seedlings contain the machinery necessary to produce fucosylated and non-fucosylated XyGs (both XXXG-type and XXGGG-type). Although the identification of wheat XyG-fucosyltransferase activity may suggest that the XyG biosynthetic mechanism may be conserved in both monocots and dicots, biochemical and enzymological demonstration is still lacking and more experimental work is needed to elucidate XyG biosynthetic mechanism in monocots. It is currently not known if the "xylosyl-glucose" backbone synthesis in grasses occurs in the Golgi and involves concomitant Glc and Xyl incorporation by XyG-xylosyltransferase and XyG-glucan synthase activities, as described in dicots [26-29]. Such a cooperative mechanism has yet to be demonstrated in grasses.

Materials and Methods

Plant Material and chemicals

Winter wheat (*Triticum aestivum* L.) seeds were grown hydroponically in the dark for 6 d at 24°C using DynaGro 7-7-7 plant fertilizer (Richmond, CA). UDP-[^{14}C]Xyl (9.78 GBq.mmol^{-1}) and GDP-[^{14}C]Fuc (7.4 GBq.mmol^{-1}) were obtained from NEN (PerkinElmer, Boston, MA). The UDP-Glc, Dowex 1X80-100 (Cl^-) ion-exchange resin, Sepharose-CL-6B and all the other chemicals were purchased from Sigma (St Louis, MO). Bio-gel P2 was from Bio-Rad. Purified pea cell wall XyG was a gift from Dr. Gordon Maclachlan (McGill University, Montreal, Canada). XyG-specific endo-β-(1,4)-glucanase (XG5, EGII, from *Aspergillus aculeatus*, 336 units/mg powder) was generously provided by Novozyme (Denmark). Tamarind XyG, rhamnogalacturonans-I (RGI, from soybean and potato), pectic galactan (from potato), arabinan (from sugar beet), AZO-xylan (Birchwood), AZO-carob galactomannan, AZO-wheat arabinoxylan, and AZO-carboxymethyl-cellulose were purchased from Megazyme International (Bray, Ireland). Oligonucleotide primers and TOP10 DH5α competent *E. coli* were from Invitrogen (Carlsbad, CA). Taq DNA polymerase, Q5 DNA polymerase, and restriction endonucleases were from New England Biolabs (Ipswich, MA). Pfu Ultra II fusion polymerase was from Agilent (Santa Clara, CA). Kapa HiFi HotStart polymerase was from Kapa Biosystems (Boston, MA). Spin columns for plasmid purification were from Epoch Biolabs (Sugar Land, TX) using the miniprep solutions and protocol from Qiagen (Valencia, CA). Gel purification was conducted using the Wizard SV gel and PCR cleanup system from Promega (Madison, WI). All primers used in this study are listed in Table 5.

Purification of XyG-specific endo-β-1,4-glucanase XG5

The purification of XyG-specific endo-β-1,4-glucanase (XG5) was carried out according to [40] with some modifications. The crude XG5 provided by Novozyme was dialyzed against 50mM acetate buffer (pH 5.0) for two days in dialysis membrane having a MW cut off of 12-14kDa (Spectrum, Houston, TX). Dialyzed filtrate was applied to a Sep-Pak® Vac Accell Plus QMA anion-exchange disposal column, 1cc/100mg, 37-55µm (Waters, Milford, MA) and the activity eluted with 50mM acetate buffer (pH 5). Fractions (0.5ml each) with high endo-β-1,4-glucanase activity were pooled and fractionated by gel permeation chromatography on a 1x30cm Superose 12 (12/300 GL) column (GE healthcare, Pittsburgh, PA). The column was eluted with 200mM sodium phosphate buffer (pH7) at a flow rate of 0.2ml/min and fractions collected every 2min. Active fractions were pooled, diluted to 1-5 units/µl, and stored at -20°C until use. Purified XG5 was tested for contaminating hydrolase activities on AZO-xylan (Birchwood), AZO-carob galactomannan, AZO-wheat arabinoxylan, and AZO-carboxymethyl-cellulose, and directly on tamarind XyG and screened for released monosaccharides. Also purified XG5 was tested for contaminant glycosidase activities on several paraphenyl-glycosides and. Under our conditions, no contaminant hydrolase and glycosidase activities were detected. However, when XG5 was tested on MLG according to [65], we detected mild β-glucan hydrolase activity, which releases mainly two diagnostic oligosaccharides, the tri-saccharide G-(1,4)-G-(1,3)-Gr and the tetra-saccharide G-(1,4)-G-(1,4)-G-(1,3)-Gr (in which G is β-D-Glc*p* and Gr is the reducing terminal residue). The release of these MLG oligosaccharides were estimated by the phenol-sulfuric acid method [66].

Golgi-enriched microsomal membranes preparation

Tissues from 6-day old etiolated wheat and pea seedlings (grown on vermiculate) were used for microsomal preparation as described earlier [67] with minor modifications. Briefly, ~25g of

tissues were harvested and ground with a mortar and pestle in 50mL of extraction buffer (0.1M HEPES-KOH pH7, 0.4M sucrose, 1mM DTT, 5mM $MgCl_2$, 5mM $MnCl_2$, 1mM phenylmethylsulphonyl fluoride, 1 tablet of Roche complete protease inhibitor cocktail). The suspension was filtered through two layers of miracloth, and the filtrate centrifuged at 3,000x*g* for 20min. The residual, ground tissue was kept at -20°C for cell wall preparation and XyG extraction (see below). The resulting supernatant was layered over 1.8M sucrose cushion buffer and centrifuged at 100,000x*g* for 60min. Total microsomal membranes located at the top of the 1.8M sucrose cushion were collected and pelleted by centrifugation at 100,000x*g* for 30min. The pellet was resuspended in 200µl extraction buffer and stored at -80ºC until use. This standard procedure usually yields membrane fractions with protein concentration of ~5-6µg/µL. Protein content was estimated using the Bradford Reagent (Sigma) and various concentrations of bovine serum albumin (BSA) as standards.

XyG-fucosyltransferase assays

Standard XyG-fucosyltransferase assay: The activity was measured as described earlier [44] with minor modifications. The reaction mixture (70µL final volume) contained the Triton X-100-solubilized enzyme from microsomes of 6-day-old wheat seedlings (40µl containing ~0.2mg protein), 100µg tamarind XyG, and 6µM GDP-[^{14}C]Fuc (65,000 cpm) or 30nM GDP-[^{3}H]Fuc (70,000 cpm). Reactions were incubated for 2h at room temperature and terminated by adding 1mL of cold 70% (v/v) ethanol and precipitated for at least 1h at -20˚C. Insoluble products were pelleted by centrifugation at 10,000x*g* (10min, 4ºC), washed three times with 1mL of cold 70% (v/v) ethanol to remove excess GDP-[^{14}C]Fuc, and the incorporation of [^{14}C]Fuc into pellets (cpm/reaction) was determined by scintillation counting using a Beckman Coulter LS 6500 counter.

Effect of pH and divalent ions on wheat XyG-fucosyltransferase: The effect of pH on wheat activity was tested using Triton X-100 extracts under the same conditions as above but using 0.1M MES-KOH buffer for pH 4 and 5, and 0.1M HEPES-KOH buffer for pH 6 and 8. The effect of 5mM divalent ions ($MnCl_2$, $MgCl_2$, $CuCl_2$, $NiCl_2$, and $ZnSO_4$) on wheat activity was tested under the same conditions as above, except that Golgi-enriched microsomes used were prepared with extraction buffer lacking any ions. Radiolabeled Fuc incorporation into pellets (cpm/reaction) was determined as described above.

Preparation of XyG oligosaccharides (XyGOs)

Lyophilized KOH extracts (8mg) were resuspended in 0.4mL of 20mM sodium acetate buffer, pH5, to which 40 units of purified XyG-specific endo-β-(1,4)-glucanase (XG5) were added. The reaction mixtures were incubated at 37°C for 16 h with stirring. To terminate the reactions, mixtures were boiled (10min) and polymers were precipitated with 70% (v/v) cold ethanol for 1 h at -20°C. After centrifugation (14,000x*g*, 10min), the supernatant was collected and ethanol removed by evaporation at 60°C. Control reactions containing XG5 enzyme were boiled immediately after adding the enzyme and then incubated at 37°C for 16 h. Released XyGOs were used directly in ESI-MS and CID-MS/MS analyses.

Electrospray ionization mass spectrometry (ESI-MS) and collision induced dissociation (CID)-MS/MS analyses

Samples (wheat XyGOs) containing 0.5mg carbohydrate were dissolved in 50% (v/v) methanol containing 0.1% (v/v) acetic acid. The sample was injected into the ESI source at a rate of 3µL/min using a Cole-Parmer 74900 syringe pump. ESI-MS spectra were acquired on an Esquire 6000 Ion Trap analyzer (Bruker Daltonics, Bremen, Germany) operated in positive ion mode with a capillary voltage 4kV, drying gas temperature 300°C, drying gas flow rate 5L/min and

nebulizer pressure 10 psi. Nitrogen was used as both the nebulizing gas and drying gas. The mass range scanned was from 200 to 1500 atomic mass units. For CID-MS/MS, the spectra were recorded using the same instrument; the parent ions ($[M+Na]^+$) were selected in the first MS spectrum, then MS/MS spectra of daughter ions were obtained using collision induced dissociation (CID) with helium as the collision gas (introduced into the system to an estimated pressure of 4 $x10^{-6}$ mbar). The amplitude of the excitation was 1 V. Instrument control and data acquisition were performed with Esquire 5.0 software.

High pH anion exchange chromatography (HPAEC) analysis

Monosaccharide composition: Xyloglucan oligosaccharides (1mg) were mixed with trifluoroacetic acid (TFA) to a final concentration of 2M in a glass vial sealed with Teflon lined cap and autoclaved for 1 h at 120°C. The hydrolysates were desalted with Bio-Rex MSZ 501 resin (Bio-Rad) before analysis by HPAEC on a CarboPac PA20 column (Thermo-Dionex). The column was eluted at a flow rate of 0.5mL/min by isocratic elution for 30 min with 2.5mM NaOH solution. Monosaccharides Fuc, Ara, Gal, Glc, and Xyl were used as standards. The standards were run before analysis of samples to make sure that their elution profiles did not change between injections.

Analysis of [^{14}C]Fuc-labeled tamarind XyG oligosaccharides: [^{14}C]radiolabeled tamarind XyGOs were prepared by digestion of [^{14}C]Fuc-tamarind XyG (produced by wheat fucosyltransferase reactions) with endoglucanase from *Trichoderma* sp. (E-CELTR, Megazyme, Bray, Ireland). [^{14}C]Fuc-tamarind XyGOs were desalted with Dowex before analysis by HPAEC on a CarboPac PA200 column (Thermo-Dionex) as described earlier [29] with some modifications. Briefly, the column was eluted at a flow rate of 0.5mL/min for 60min at 30°C with an isocratic solution of 100mM NaOH containing 22mM sodium acetate; [^{14}C]radiolabeled

samples were injected in several repetitions to collect enough material for cpm counting. Known XyGO standards (*i.e.*, XXXG, XXFG, XLFG, XLLG, XLXG/XXLG) were included with [^{14}C]radiolabeled samples as a control to make sure that their elution profiles did not change between injections.

Identification of putative wheat fucosyltransferase (FUT) genes and phylogenetic analysis

Putative wheat FUTs were identified from EST databases, sequence reads from the 5X wheat genome (http://www.cerealsdb.uk.net/), and the partially assembled 5X wheat genome [68]. We developed two *in-house* scripts: one was used to screen wheat transcriptomes and the second for phylogenetic analysis. Both scripts were described in [69]. Briefly, these scripts perform a tBlastn (NCBI) search using rice and Arabidopsis GT protein sequences as queries and collect all the hits (E<0.05). After removal of redundancy (same accession number), the ESTs were merged into unique contigs using the CAP3 assembly program [70]. For the identification of contigs corresponding to various regions of the same gene sequence, it was necessary to manually perform several alignments using the ClustalW program and compare similarities with the closest full-length rice gene sequences. This step reduced the number of candidate wheat sequences and allowed the identification of start and stop codons of the wheat FUT genes. Additional wheat GT37 members were identified from the Roche 454 wheat genome sequence (http://www.cerealsdb.co.uk) using wheat FUT nucleotide sequences as a query. Obtained sequences were assembled using the built-in CAP3 program. Assembly and analysis of the 5X wheat genome allowed for the identification of additional putative wheat FUTs using Brachypodium gene identifiers as a query ([68]; http://mips.helmholtz-muenchen.de/plant/wheat/uk454survey/index.jsp). More wheat FUT sequences were found at Phytozome v12.1.6 (the Plant Comparative Genomics portal of the Department of Energy's Joint

Genome Institute), under early Release Species, (https://phytozome.jgi.doe.gov/pz/portal.html#!search?show=BLAST&method=Org_Taestivum_er). All hits above or equal to the score 920 (E≤2.5e-83) were collected. The final list of sequences was checked for the presence of the FUT domain using the CCD program at NCBI through the BLASTp program [71]. Rice GT37 members in the CAZy database were downloaded from GenBank. Putative full-length FUT protein sequences from rice, Arabidopsis, and wheat were used in the phylogenetic analysis along with partial sequences (ESTs or contigs) from wheat. Protein sequences were aligned using Muscle multiple sequence alignment [72]. Phylogenetic analysis was performed in the Phylogeny.fr platform (http://www.phylogeny.fr/ [73]) using 'One Click' mode, which uses pipeline chaining of the following programs MUSCLE for multiple alignment [72], PhyML for tree building [74], and TreeDyn for tree rendering [75]. Default parameters were used for the phylogenetic analysis including Maximum-likelihood tree construction to infer phylogenies, which is commonly accepted as the most accurate approach in molecular phylogenetics [76]. PhyML is run with the aLRT statistical test [77] of branch support (to infer bootstrap values) is based on an approximation of the standard Likelihood Ratio Test. The number of bootstrap replicates is limited to 100. However, to confirm the stability of the phylogenetic results, we run 'A la Carte' mode using several different programs with various options. All methods output the same trees with branch supports that are highly correlated.

Cloning of TaFUT-F and TaFUT-O genes

The original EST designated TaFUT-F (BU099714, full tillering stage drought stressed cDNA library from the USDA) was 667bp long and missing sequences from both the 3' and 5' ends. The 3' end sequence and 3' untranslated region (UTR) of *TaFUT-F* were verified by 3' Rapid Amplification of cDNA ends (RACE) using the GeneRacer kit (Invitrogen). Two micrograms of

619 total RNA from wheat roots was reverse transcribed using SuperScriptIII reverse transcriptase
620 with the oligo(dT) primer including an adaptor sequence included with the kit. First round PCR
621 was performed with a forward primer in the EST (5'-GCGGAGATATATCTGCTCAGCCTC-
622 3') and the oligo(dT) adaptor primer using 2µL of cDNA template. Touchdown (TD)-PCR was
623 performed using with the following program: 96°C for 3min; 20 cycles of 96°C for 15s, 65°C for
624 15s decreasing by 0.5°C each cycle, 72°C for 90s; 20 cycles of 96°C for 15s, 55°C for 15s, 72
625 for 90s; and final extension at 72°C for 5 min. Second round PCR was performed using 1µL of
626 the 1st round PCR product as template, a forward nested primer in the EST (5'-
627 GTGATGTTCAAGCCGGACA-3') and the nested 3' primer included in the kit. Cycling
628 conditions were the same as first round PCR. The 5' end was cloned through RNA-ligase
629 mediated RACE (RLM-RACE) using the GeneRacer kit (Invitrogen). Total RNA template was
630 made according to manufacturer's instructions. Reverse transcription was conducted as for 3'
631 RACE. First round PCR was conducted on the reverse transcribed RNA using the GeneRacer 5'
632 forward primer and a reverse target specific primer (TSP) located in the EST (5'-
633 AATGGCTCGCAGAACAGCTC-3'). Touchdown-PCR was conducted using Kapa HiFi
634 polymerase and the same program as above except the annealing temperature started at 72°C and
635 touched down to 62°C. Nested PCR was performed using 1µL of the 1st round PCR product as
636 template and the 5' GeneRacer nested primer and a nested TSP (5'-
637 ACATGGCGGACTGGTACCTGCTGTG-3') using the same PCR program. The full-length
638 *TaFUT-F* cDNA was then cloned from cDNA generated for 5' RACE using forward primer (5'-
639 ATGCTGCGACGGGACGTC-3') and reverse primer (5'-GCACACGCCACCAGGTTTC-3') in
640 a 50µL reaction containing 2µL cDNA template, 5µL 10X reaction buffer, 250µM each dNTP,
641 0.5µM each primer, and 1µL Pfu Ultra II Fusion DNA polymerase using the following program:

642 94°C for 3min; 30 cycles of 94°C for 30s, 57°C for 30s, 72°C for 90s; and a final extension at
643 72°C for 5 min.

644 For *TaFUT-O*, the second exon was found by searching the wheat genome with the gene
645 identifier "*Bradi3g58030.*1" ([68],
646 http://mips.helmholtzmuenchen.de/plant/wheat/uk454survey/index.jsp). Primers were designed
647 specifically from the entry "Traes_Bradi3g58030.1_000002_B." The full-length *TaFUT-O*
648 transcript was amplified from cDNA prepared for 5' RACE as a template (described above)
649 using a forward primer designed from Brachypodium homolog, *Bradi3g58030*, 5'-
650 ATGGACCTCAAGGAGCGGATCC-3', and a reverse primer (designed in the 3'UTR) 5'-
651 TTGGATAGGAAATACGCACCACATC-3' in a 25µL PCR reaction containing 2µL cDNA
652 template, 0.8µM each primer, 250µM each dNTP, 5µL of 5X Q5 buffer, and 1U of Q5 Hot-start
653 DNA polymerase. Touchdown PCR was conducted with the following program: 98°C for 30s;
654 20 cycles of 98°C for 10s, 72°C for 20s decreasing by 0.5°C each cycle, 72°C for 1 min; 20
655 cycles of 98°C for 10s, 62°C for 20s, 72 for 1 min; and final extension at 72°C for 5 min.

656 *TaFUT-D* was cloned from cDNA produced from wheat root RNA (prepared as described
657 above for 3' RACE) using Kapa HiFi HotStart polymerase. The reaction was set up according to
658 manufacturer's instructions using forward primer (5'-ATGGGGAGGAGCGGCG-3') and
659 reverse primer (5'-CAGCTACAACCGAGTTTCATTT-3') and the following PCR program:
660 95°C for 3 min; 30 cycles of 98°C for 20s, 65°C for 15s, 72°C for 60s; and a final extension at
661 72°C for 3 min.

662 *Expression profiling of wheat FUT genes*

663 Total RNA was isolated from the roots and coleoptiles of etiolated wheat seedlings using Direct-
664 zol RNA Miniprep (Zymo Research, Irvine, CA). Two micrograms of total RNA was reverse

transcribed with an oligo(dT) primer using the Applied Biosystems High Capacity cDNA Reverse Transcription kit according to the manufacturer's instructions. Genomic DNA was extracted from shoot tissues using a CTAB extraction method [78]. Complementary DNA (cDNA) from roots and shoots of etiolated wheat was used for PCR screening of nine *TaFUT* genes. Gene-specific primers were designed to amplify products from these *TaFUT* genes ranging in size from 220-398bp (Table 5). The products were confirmed through sequencing. Template cDNA was prepared as described in the previous section. Products were amplified in a 20µL PCR reaction containing 1-2µL cDNA template (normalized using control primers), 1µM each primer, 250mM each dNTP, 2µL standard Taq buffer, and 1U *Taq* DNA polymerase. Cycling conditions were as follows: 96°C for 2min; 25 cycles of 96°C for 15s, 58°C for 15s, 72°C for 40s; and a final extension at 72°C for 7min. The annealing temperatures for *TaFUT-O* and Ta54227 were 64°C and 70°C, respectively. Control primers were for *Ta54227*, a gene encoding a cell division control protein that is a member of the AAA-superfamily of ATPases [79]. It was chosen as a control based on its stable expression between different tissue types and outperformance of common controls such as actin or ubiquitin [79].

Expression in Pichia pastoris cells

Transformation of *Pichia pastoris* was carried out according to the manufacturer's manual (Invitrogen) with minor modifications. A colony of *Pichia pastoris* strain X-33 was picked from a Yeast Peptone Dextrose [YPD; 1% (w/v) yeast extract, 2% (w/v) peptone, 2% (w/v) agar] plate and grown in 5mL liquid YPD in a 50mL conical tube overnight at 28°C with constant shaking (220 rpm). Five-hundred microliters of this culture was used to inoculate 250mL fresh YPD in a 1L flask. Cells were grown to an OD600 ~1 (~10 hrs) and harvested by centrifugation at 3000x*g* for 5 min. The pellet was re-suspended in 200mL ice-cold sterile water and centrifuged. The

688 pellet was then re-suspended in 100mL ice-cold sterile water and centrifuged again. The pellet
689 was re-suspended in 10mL of ice cold 1M sorbitol and centrifuged again, and the final pellet was
690 resuspended in 300µL 1M sorbitol. Competent cells were kept on ice and used for
691 electroporation the same day.

692 Constructs of His-tagged FUT genes in pPICZa were prepared for electroporation as follows.
693 A single construct was grown overnight in 18mL LB (6 x 3mL cultures) containing 100 µg/mL
694 Zeocin, and bacteria cells were used for plasmid DNA preparation using the standard miniprep
695 procedure (Qiagen). The purified plasmid was precipitated by adding 1/10th volume 3M sodium
696 acetate and 2.5 volume 100% cold ethanol, left overnight at -20°C, recovered by centrifugation
697 at 14,000x*g* for 20 min at 4°C, washed once with 200µL cold 70% ethanol, and re-suspended in
698 15µL (typical yield is ~17µg of DNA). Ten micrograms of the plasmid was linearized with 10U
699 of *Pme*I in a 10µL volume, and 1µL was used to monitor the status of the linearization on a DNA
700 gel.

701 Pichia competent cells (80µL) were combined with the linearized plasmid and allowed to
702 incubate on ice for five minutes prior to electroporation. The cells were pulsed at 1.8kV, 200
703 ohms, 25 µF in a Gene Pulser II Electroporation System (BioRad). Following electroporation,
704 1mL of 1M sorbitol was added to the electroporation cuvette and the contents were transferred to
705 a 15mL conical tube and incubated for 2 h at 28°C. Cells were plated on YPDS [1% (w/v) yeast
706 extract, 2% (w/v) peptone, 1M sorbitol, 2% (w/v) agar] containing 100-200µg/mL Zeocin. After
707 2-3 days of incubation, ten colonies were picked and grown in 3mL YPD containing 100µg/mL.

708 Two to five colonies for each construct were chosen for the production of the proteins. First,
709 100 µL of a colony's glycerol stock was added to 15mL BMGY [1% (w/v) yeast extract, 2%
710 (w/v) peptone, 100mM potassium phosphate buffer pH 6, 1.34% (w/v) yeast nitrogen base,

711 $4x10^{-5}$% (w/v) biotin, 1% (v/v) glycerol] and grown at 28°C overnight with constant shaking
712 (220 rpm) until the OD600 was between 2 and 6. To initiate the induction of protein production,
713 Pichia cells were harvested by centrifugation at 3,000x*g* for 10 min and re-suspended to an
714 OD600 of 1 in 30-50mL BMMY [1% (w/v) yeast extract, 2% (w/v) peptone, 100mM potassium
715 phosphate buffer pH 6, 1.34% (w/v) yeast nitrogen base, $4x10^{-5}$% (w/v) biotin, 0.5% (v/v)
716 methanol]. Methanol was added every 24 h to a final concentration of 0.5% (v/v) to maintain the
717 induction. One mL was taken from the culture each day to monitor the level of protein
718 expression using western blot analysis. After 4 days of induction, microsomes were prepared as
719 described earlier [31] with minor modifications. Cells were pelleted by centrifugation at 3,000x*g*
720 for 15 min, re-suspended in 10mL extraction buffer (EB) [100mM HEPES-KOH pH 7, 0.2M
721 sucrose, 1mM dithiothreitol (DTT), 5mM $MgCl_2$, 5mM $MnCl_2$, 1mM
722 phenylmethanesulphonylfluoride (PMSF)], pelleted again, and resuspended in 5mL EB
723 containing 1x complete protease inhibitor (Roche) and 50 µL RPI protease inhibitor cocktail VI
724 (concentrations in vial: 200mM AEBSF, HCl; 10mM Bestatin; 3mM E-64; 2mM Pepstatin A;
725 2mM Leupeptin; 500mM 1,10 phenanthroline). Transgenic Pichia cells were broken in 15mL
726 conical tubes by adding ~2mL glass beads (425-600 µm diameter) and vortexing seven times, 30
727 s each time. Tubes were inverted each time while vortexing and kept on ice at least 1.5 min
728 between each vortexing. Broken cells were centrifuged at 3,000x*g* at 4°C for 15 min to collect
729 beads and remove cell debris. The supernatant was centrifuged at 100,000x*g* for 1 h at 4°C to
730 collect microsomal membranes, and the pellet was re-suspended in ~400µL EB. This procedure
731 yielded membrane fractions ranging from 1 to 5 µg/mL of protein as determined by a Bradford
732 assay.

733 *GenBank accession numbers of cloned wheat FUT genes*

734 The nucleotide sequences of *TaFUT-D*, *TaFUT-F*, *and TaFUT-O* have been assigned the

735 following GenBank accession numbers: MN529249, MN529250, MN529251, respectively.

References

1. Hayashi, T. (1989) Xyloglucan in the primary cell walls. Annu. Rev. Plant Physiol. Plant Mol. Biol., 40: 139-168
2. Carpita, NC. and Gibeaut, DM. (1993) Structural models of primary cell walls in flowering plants: consistency of molecular structure with the physical properties of the walls during growth. Plant J., 3: 1-30
3. Bootten, TJ., Harris, PJ., Melton, LD., Newman, RH. (2004) Solid-state 13C-NMR spectroscopy shows that the xyloglucans in the primary cell walls of mung beans (Vigna radiata L.) ocuur in different domains: a new model for xyloglucan-cellulose interactions in the cell wall. J. Exp. Bot., 55: 571-583
4. Park, YB. and Cosgrove, DJ. (2012) A revised architecture of primary cell walls based on biomechanical changes induced by substrate-specific endoglucanases/ Plant Physiol., 158: 1933-1943
5. Hayashi, T. and Kaida, R. (2011) Functions of xyloglucan in plant cells. Mol. Plant, 4: 17-24
6. Gibeaut, DM., Pauly, M., Bacic, A., Fincher, GB. (2005) Changes in cell wall polysaccharides in developing barley (Hordeum vulgare) coleoptiles. Planta, 221: 729-738
7. Vincken, JP., York, WS., Beldman, G., Voragen, AG. (1997) Two general branching patterns of xyloglucan, XXXG and XXGG. Plant Physiol., 114: 9-13
8. Stephen, C. and Fry, WSY. (1993) An unambiguous nomenclature for xyloglucan-derived oligosaccharides. Physiol Plant 89: 1-3.
9. Tuomivaara, ST., Yaoi, K., O'Neill, MA., York, WS. (2015) Generation and structural validation of a library of diverse xyloglucan-derived oligosaccharides, including an update on xyloglucan nomenclature. Carbohydr Res., 402: 56–66
10. Mabusela, WT., Stephen, AM., Rodgers, AL., Gerneke, DA. (1990) A highly substituted glucan that coats the seeds of Helipterum eximium. Carbohydr Res., 203: 336–340
11. Hoffman, M., Jia, Z., Peña, MJ., Cash, M., Harper, A., Blackburn, AR., et al.(2005) Structural analysis of xyloglucans in the primary cell walls of plants in the subclass Asteridae. Carbohydr Res., 340: 1826–1840
12. Buckeridge, MS., Crombie, HJ., Mendes, CJ., Reid, JS., Gidley, MJ., Vieira, CC. (1997) A new family of oligosaccharides from the xyloglucan of Hymenaea courbaril L. (Leguminosae) cotyledons. Carbohydr. Res., 303: 233–237

13. Kato, Y., Iki, K., Matsuda, K. (1981) Cell-wall Polysaccharides of Immature Barley Plants. II. Characterization of a Xyloglucan. Agric. Biol. Chem., 45: 2745–2753

14. Kato, Y., Ito, S., Iki, K., Matsuda, K. (1982) Xyloglucan and β-D-glucan in cell walls of rice seedlings. Plant Cell Physiol., 23: 351–364

15. Shibuya, N. and Iwasaki, T. (1985) Structural features of rice bran hemicellulose. Phytochemistry, 24: 285–289.

16. Sims, IM., Middleton, K., Lane, AG., Cairns, AJ., Bacic, A. (2000) Characterization of extracellular polysaccharides from suspension cultures of members of the Poaceae. Planta, 210: 261–268

17. Jia, Z., Cash, M., Darvill, AG., York, WS. (2005) NMR characterization of endogenously *O*-acetylated oligosaccharides isolated from tomato (*Lycopersicon esculentum*) xyloglucan. Carbohydr Res., 340: 1818–1825

18. Brennan, M. and Harris, PJ. (2011) Distribution of fucosylated xyloglucans among the walls of different cell types in monocotyledons determined by immunofluorescence microscopy. Molecular Plant 4:144-156

19. McDougall, GJ. and Fry, SC. (1994) Fucosylated Xyloglucan in Suspension-Cultured Cells of the Graminaceous Monocotyledon, Festuca arundinacea. J Plant Physiol., 143: 591–595

20. Liu, L., Paulitz, J., Pauly, M. (2015) The presence of fucogalactoxyloglucan and its synthesis in rice indicates conserved functional importance in plants. Plant Physiol., 168: 549–560

21. Jia, Z., Qin, Q., Darvill, AG., York, WS. (2003) Structure of the xyloglucan produced by suspension-cultured tomato cells. Carbohydr. Res., 338: 1197–1208;

22. Schultink, A., Liu, L., Zhu, L., Pauly M. (2014) Structural Diversity and Function of Xyloglucan Sidechain Substituents. Plants, 3: 526-542

23. Peña, MJ., Kong, Y., York, WS., O'Neill, MA. (2012) A galacturonic acid-containing xyloglucan is involved in Arabidopsis root hair tip growth. Plant Cell., 24: 4511-24

24. Jensen, JK., Schultink, A., Keegstra, K., Wilkerson, CG., Pauly, M. (2012) RNA-Seq analysis of developing nasturtium seeds (Tropaeolum majus): identification and characterization of an additional galactosyltransferase involved in xyloglucan biosynthesis. Mol Plant., 5: 984–992.

25. Kong, Y., Peña, MJ., Renna, L., Avci, U., Pattathil, S., Tuomivaara, ST., Li, Z., Reiter, WD., Brandizzi, F., Hahn, MG., Darvill, AG., York, WS., O'Neill, MA. (2015) Galactose-

798 Depleted Xyloglucan Is Dysfunctional and Leads to Dwarfism in Arabidopsis. Plant Physiol.,
799 167: 1296–1306
800 26. Ray, PM. (1980) Cooperative action of beta-glucan synthetase and UDP-xylose xylosyl
801 transferase of Golgi membranes in the synthesis of xyloglucan-like polysaccharide. Biochim
802 Biophys Acta., 629: 431–444.
803 27. Hayashi, T. and Matsuda, K. (1981) Biosynthesis of xyloglucan in suspension-cultured
804 soybean cells. Occurrence and some properties of xyloglucan 4-beta-D-glucosyltransferase
805 and 6-alpha-D-xylosyltransferase. J Biol Chem., 256: 11117–11122.
806 28. Gordon, R. and Maclachlan, G. (1989) Incorporation of UDP-[C]Glucose into Xyloglucan by
807 Pea Membranes. Plant Physiol., 91: 373–378.
808 29. Faik, A, Bar-Peled, M., DeRocher, AE., Zeng, W., Perrin, RM., Wilkerson, C., et al. (2000)
809 Biochemical characterization and molecular cloning of an alpha-1,2-fucosyltransferase that
810 catalyzes the last step of cell wall xyloglucan biosynthesis in pea. J Biol Chem., 275: 15082–
811 15089
812 30. Perrin, RM., DeRocher, AE., Bar-Peled, M., Zeng, W., Norambuena, L., Orellana, A., et al.
813 (1999) Xyloglucan fucosyltransferase, an enzyme involved in plant cell wall biosynthesis.
814 Science, 284: 1976–1979
815 31. Faik, A., Price, NJ., Raikhel, NV., Keegstra, K. (2002) An Arabidopsis gene encoding an
816 alpha-xylosyltransferase involved in xyloglucan biosynthesis. Proc Natl Acad Sci U S A., 99:
817 7797–7802
818 32. Cavalier, DM. and Keegstra, K. (2006) Two xyloglucan xylosyltransferases catalyze the
819 addition of multiple xylosyl residues to cellohexaose. J Biol Chem., 281: 34197–34207
820 33. Zabotina, OA., van de Ven, WTG., Freshour, G., Drakakaki, G., Cavalier, D., Mouille, G., et
821 al. (2008) Arabidopsis XXT5 gene encodes a putative alpha-1,6-xylosyltransferase that is
822 involved in xyloglucan biosynthesis. Plant J Cell Mol Biol., 56: 101–115
823 34. Vuttipongchaikij, S., Brocklehurst, D., Steele-King, C., Ashford, DA., Gomez, LD.,
824 McQueen-Mason, SJ. (2012) Arabidopsis GT34 family contains five xyloglucan α-1,6-
825 xylosyltransferases. New Phytol., 195: 585–595
826 35. Zabotina, OA., Avci, U., Cavalier, D., Pattathil, S., Chou, Y-H., Eberhard, S., Danhof, L.,
827 Keegstra, K., Hahn MG. (2012) Mutations in multiple *XXT* genes of Arabidopsis reveal the
828 complexity of xyloglucan biosynthesis. Plant Physiol., 159: 1367-1384

829 36. Madson, M., Dunand, C., Li, X., Verma, R., Vanzin, GF., Caplan, J., et al. (2003) The *MUR3*
830 gene of Arabidopsis encodes a xyloglucan galactosyltransferase that is evolutionarily related
831 to animal exostosins. Plant Cell, 15: 1662–1670.
832 37. Cocuron, J-C., Lerouxel, O., Drakakaki, G., Alonso, AP., Liepman, AH., Keegstra, K., et al.
833 (2007) A gene from the cellulose synthase-like C family encodes a beta-1,4 glucan synthase.
834 Proc Natl Acad Sci U S A., 104: 8550–8555
835 38.Watanabe, T., Shida, M., Murayama, T., Furuyama, Y., Nakajima, T., Matsuda, K., Kainuma,
836 K. (1984) Xyloglucan in cell walls of rice hull. Carbohydr. Res., **129**: 229–24
837 39. Hsieh, YS. and Harris, PJ. (2009) Xyloglucans of monocotyledons have diverse
838 structures. Mol Plant **2**: 943–965
839 40. Pauly, M., Andersen, LN., Kauppinen, S., Kofod, LV., York, WS., Albersheim, P., et al.
840 (1999) A xyloglucan-specific endo-beta-1,4-glucanase from Aspergillus aculeatus: expression
841 cloning in yeast, purification and characterization of the recombinant enzyme. Glycobiology,
842 9: 93–100
843 41. Hayashi, T. and Maclachlan, G. (1984) Pea xyloglucan and cellulose□: I. Macromolecular
844 organization. Plant Physiol., 75: 596–604
845 42. Domon, B. and Costello, CE. (1988) A systematic nomenclature for carbohydrate
846 fragmentations in FAB-MS/MS spectra of glycoconjugates. Glycoconj J., 5: 397–409
847 43. Reis, A., Pinto, P., Evtuguin, DV., Neto, CP., Domingues, P., Ferrer-Correia, AJ., et al.
848 (2005) Electrospray tandem mass spectrometry of underivatised acetylated xylo-
849 oligosaccharides. Rapid Commun Mass Spectrom RCM., 19: 3589–3599
850 44. Shipp, M., Nadella, R., Gao, H., Farkas, V., Sigrist, H., Faik, A.(2008) Glyco-array
851 technology for efficient monitoring of plant cell wall glycosyltransferase activities.
852 Glycoconj. J., 25: 49–58
853 45. Darvill, A.G., McNeil, M., Albersheim, P. (1978) Structure of Plant Cell Walls VIII. A New
854 Pectic Polysaccharide. Plant Physiol., 62: 418-422
855 46. Vincken, J-P., Beldman, G., Niessen, WMA., Voragen, AGJ. (1996) Degradation of apple
856 fruit xyloglucan by endoglucanase. Carbohydr. polym., 29: 75-85
857 47. Faik, A., Chileshe, C., Sterling, J., Maclachlan, G. (1997) Plant Physiol., 114: 245-254
858 48. Hisamatsu, M., Impallomeni, G., York, WS., Albersheim, P., and Darvill, AG. (1991)
859 Carbohydr. Res., 211: 117-129

860 49. Liptay, A. and Davidson, D. (1972) Growth of the Barley Coleoptile. I. Its Relationship to
861 Cell Number and Length in Normal and γ-Irradiated Seedlings. Am J Bot., 59: 266–269
862 50. Carpita, NC., Defernez, M., Findlay, K., Wells, B., Shoue, DA., Catchpole, G., et al. (2001)
863 Cell wall architecture of the elongating maize coleoptile. Plant Physiol., 127: 551–565
864 51. Peña, MJ., Darvill, AG., Eberhard, S., York, WS., O'Neill, MA. (2008) Moss and liverwort
865 xyloglucans contain galacturonic acid and are structurally distinct from the xyloglucans
866 synthesized by hornworts and vascular plants. Glycobiology **18**: 891–904
867 52. Sakurai, N. and Masuda, Y. (1978) Auxin-induced changes in barley coleoptile cell wall
868 composition. Plant Cell Physiol., 19: 1217–1223
869 53. Shewry, PR. editor. Barley: Genetics, Biochemistry, Molecular Biology and Biotechnology.
870 Wallingford, Oxon, UK: Oxford University Press; 1992
871 54. Rose, JKC., Braam, J., Fry, SC., Nishitani, K. (2002) The XTH family of enzymes involved
872 in xyloglucan endotransglucosylation and endohydrolysis: current perspectives and a new
873 unifying nomenclature. Plant Cell Physiol., 43: 1421–1435
874 55. Shibuya, N. and Misaki, A. (1978) Structure of hemicelluloses isolated from rice endosperm
875 cell wall: mode of linkages and sequences in xyloglucan, β-Glucan and arabinoxylan. Agric.
876 Biol. Chem., 42: 2267–2274.
877 56. Inouhe, M., Yamamoto, R., Masuda, Y. (1984) Auxin-induced changes in the molecular
878 weight distribution of cell wall xyloglucans in Avena Coleoptile. Plant Cell Physiol., 25:
879 1341–1351
880 57. Kulkarni, AR., Pattathil, S., Hahn, MG., York, WS., O'Neill, MA. (2012) Comparison of
881 Arabinoxylan Structure in Bioenergy and Model Grasses. Ind. Biotechnol., 8: 222–229
882 58. Sarria, R., Wagner, TA., O'Neill, MA., Faik, A., Wilkerson, CG., Keegstra, K., et al. (2001)
883 Characterization of a family of Arabidopsis genes related to xyloglucan fucosyltransferase1.
884 Plant Physiol., 127: 1595–1606
885 59. Wu, Y., Williams, M., Bernard, S., Driouich, A., Showalter, AM., Faik, A. (2010) Functional
886 identification of two nonredundant Arabidopsis alpha(1,2)fucosyltransferases specific to
887 arabinogalactan proteins. J Biol Chem., 285: 13638–13645
888 60. Vanzin, GF., Madson, M., Carpita, NC., Raikhel, NV., Keegstra, K., Reiter, W-D. (2002)
889 The *mur2* mutant of *Arabidopsis thaliana* lacks fucosylated xyloglucan because of a lesion in
890 fucosyltransferase AtFUT1. Proc Natl Acad Sci U S A., 99: 3340–3345

891 61. Del Bem, LE. and Vincentz, MG. (2010) Evolution of xyloglucan-related genes in green
892 plants. BMC Evol. Biol., 10: 341
893 62. Kostlánová, N., Mitchell, EP., Lortat-Jacob, H., Oscarson, S., Lahmann, M., Gilboa-Garber,
894 N., et al. (2005) The fucose-binding lectin from Ralstonia solanacearum. A new type of beta-
895 propeller architecture formed by oligomerization and interacting with fucoside,
896 fucosyllactose, and plant xyloglucan. J. Biol. Chem., 280: 27839–27849
897 63. Wen, F., Celoy, RM., Nguyen, T., Zeng, W., Keegstra, K., Immerzeel, P., et al. (2008)
898 Inducible expression of Pisum sativum xyloglucan fucosyltransferase in the pea root cap
899 meristem, and effects of antisense mRNA expression on root cap cell wall structural integrity.
900 Plant Cell Rep., 27: 1125–1135
901 64. Lampugnani, ER., Moller, IE., Cassin, A,. Jones, DF., Koh, PL, Ratnayake, S., et al (2013).
902 In vitro grown pollen tubes of Nicotiana alata actively synthesise a fuco.sylated xyloglucan.
903 PloS One, 8: e77140
904 65. McCleary, BV. and Glennie-Holmes, M. (1985) Enzymatic quantification of (133)(134)-□-
905 d-glucan in barley and malt. Journal of the Institute of Brewing 91: 285–295
906 66. DuBois, M., Gilles, KA., Hamilton, JK., Rebers, PA., Smith, F. (1956) Colorimetric Method
907 for Determination of Sugars and Related Substances. Anal Chem., 28: 350–356
908 67. Zeng, W., Chatterjee, M., Faik, A. (2008) UDP-Xylose-stimulated glucuronyltransferase
909 activity in wheat microsomal membranes: characterization and role in
910 glucurono(arabino)xylan biosynthesis. Plant Physiol., 147: 78–91
911 68. Brenchley R, Spannagl M, Pfeifer M, Barker GLA, D'Amore R, Allen AM, et al. (2012)
912 Analysis of the bread wheat genome using whole-genome shotgun sequencing. Nature, 491:
913 705–710
914 69. Faik, A., Abouzouhair, J., Sarhan, F. (2006) Putative fasciclin-like arabinogalactan-proteins
915 (FLA) in wheat (Triticum aestivum) and rice (Oryza sativa): identification and bioinformatic
916 analyses. Mol. Genet. Genomics, 276: 478–494
917 70. Huang, X. and Madan, A. (1999) CAP3: A DNA sequence assembly program. Genome Res.,
918 9: 868–877
919 71. Marchler-Bauer, A., Lu, S., Anderson, JB., Chitsaz, F., Derbyshire, MK., DeWeese-Scott, C.,
920 et al. (2011) CDD: a Conserved Domain Database for the functional annotation of proteins.
921 Nucleic Acids Res., 39: D225–229

922 72. Edgar, RC. (2004) MUSCLE: multiple sequence alignment with high accuracy and high
923 throughput. Nucleic Acids Res., 32: 1792–1797
924 73. Dereeper, A., Guignon, V., Blanc, G., Audic, S., Buffet, S., Chevenet, F., Dufayard, JF.,
925 Guindon, S., Lefort, V., Lescot, M., Claverie, JM., Gascuel, O. (2008) *Phylogeny.fr: robust*
926 *phylogenetic analysis for the non-specialist*. Nucleic Acids Res., 1: 36 (Web Server
927 issue):W465-9
928 74. Guindon, S. and Gascuel,O. (2003) A simple, fast and accurate algorithm to estimate larges
929 phylogenies by maximum likelihood. Syst. Biol., 52, 696–704
930 75. Chevenet, F., Brun, C., Banuls, A.L., Jacq, B., Christen, R. (2006) TreeDyn: towards
931 dynamic graphics and annotations for analyses of trees. BMC Bioinformatics, 7, 439
932 76. Kuhner, M.K. and Felsenstein, J. (1994) A simulation comparison of phylogeny algorithms
933 under equal and unequal evolutionary rates. Mol. Biol. Evol., 11, 459–468
934 77. Anisimova, M. and Gascuel, O. (2006) Approximate likelihood ratio test for branches: a fast,
935 accurate and powerful alternative. Syst. Biol., 55, 539–552
936 78. Weigel, D. and Glazebrook, J. (2002) Arabidopsis: A Laboratory Manual. CSHL Press.
937 79. Paolacci, AR., Tanzarella, OA., Porceddu, E., Ciaffi, M. (2009) Identification and validation
938 of reference genes for quantitative RT-PCR normalization in wheat. BMC Mol. Biol., 10: 11
939
940
941

942 **Table 1**: Monosaccharide composition of wheat XyG oligosaccharides (XyGOs) released from
943 KOH-extracts of wheat cell walls by digestion with XyG-specific endoglucanase (XG5 from
944 *Aspergillus aculeatus*). KOH-extracts were prepared from root and coleoptile cell walls.
945 Released wheat XyG Oligosaccharides were hydrolyzed with 2M TFA (120°C, 1h) and the
946 released monosaccharides were desalted and then analyzed by HPAEC on a CarboPac PA20
947 column (Dionex). The values are the averages of triplicate analyses plus/minus standard
948 deviation (SE). ND stands for not detected. Pea XyG oligosaccharides were prepared from
949 purified XyG that was treated with XG5.

	Wheat roots	Wheat shoots	Purified pea XyG
		(mol %)	
Glucose	60 ±2	63 ±2	45±2
Xylose	26 ±1	28 ±1	37 ±1
Arabinose	8 ±1	6 ±1	Traces
Galactose	5 ±1	3 ±1	10 ±1
Fucose	0.5 ±0.1	ND	6 ±1
Glucose:xylose ratio	2.30	2.25	1.22
Glc:Xyl:Gal:Fuc ratio	120:52:16:1	21:9:1:0	7.5:6:1.7:1

950

951

952 **Table 2**: Transfer of [^{14}C]radiolabeled fucose ([^{14}C]Fuc) from GDP-[^{14}C]Fuc to tamarind XyG
953 by Triton X-100-extracts from microsomes of etiolated wheat and pea seedlings. Detergent-
954 soluble proteins from wheat (0.2mg/reaction) or pea (0.36mg/reaction) were incubated with
955 100µg tamarind XyG and GDP-[^{14}C]fucose (65,000cpm) for 1h at room temperature, and the
956 reactions were stopped by precipitation with 1mL 70% (v/v) ethanol. [^{14}C]radiolabel
957 incorporation (expressed as pmol fucose/h/mg protein) was measured as described in Materials
958 and Methods section. The values are from experiments repeated at least five times. Deviations
959 represent standard deviation (SE).

Tissues	[^{14}C]Fuc incorporation	
	No tamarind XyG	Plus tamarind XyG
	(pmol/h/mg protein)	
Wheat coleoptile	10.3±1.5	11.3±2.5
Wheat root	3.4±1.5	31±1
Pea hypocotyl	8.5 ±2	306 ±10

960

961

962 **Table 3:** Data available in the wheat Database.

Data type	**Description**
Sequences	https://www.cerealsdb.uk.net/cerealgenomics/ A draft wheat genome assembly based on 5x coverage of 454 reads (85 Gigabases of genomic 454 sequences) of Chinese Spring
EST sequences	Functional Genomics of Abiotic Stress (FGAS) project (73,521 quality-filtered ESTs from 11 cDNA libraries constructed from wheat plants exposed to various abiotic stresses and at different developmental stages). Cultivar Norstar and two other wheat lines (CI14106 and PI178383)
EST sequences	National Science Foundation-DuPont wheat EST sequencing program (NCBI)
EST and protein sequences	https://phytozome.jgi.doe.gov/pz/portal.html#!search?show=BLAST&method=Org_Taestivum_er Phytozome website under Early Release Species

963

964

965 **Table 4**: List of wheat members of CAZy GT37 family identified by our bioinformatics
966 approach (see Materials and Methods for details) and found in Phytozome database. Rice
967 homologs are also listed. The gene highlighted in red were cloned in this work.

Identified by our approach (including homeologs)	ID in Phytozome (including homeologs)	Closest rice homolog	Predicted size (amino acids)	Full-length
TaFUT-A-1 TaFUT-A-2 TaFUT-A-3	Not present	Os02g0763200	576	Yes
TaFUT-B	Traes_2AL_07BFC11CA.1	Os04g0449100	544	Yes
TaFUT-C	Traes_4DS_37A53FCC2.1 Traes_4BS_233289BB6.1	Os06g0212600	561	Yes
TaFUT-D	Traes_6DL_E724AD52E.2 Traes_6BL_2981FD934.1	Os02g0763900	570	Yes
TaFUT-E	Traes_7DS_854E2AD57.2	Os06g0211700	521	No
TaFUT-F	Not present	Os06g0212300 Os06g0212400	589	Yes
TaFUT-G	Not present	Os06g0212100	279	No
TaFUT-H	Traes_2AL_5A666899B.1	Os02g0275200	563	Yes
TaFUT-I	Traes_6DL_B04B4C48D.1	Os02g0764200 (OsMUR2)	214	No
TaFUT-J	Traes_1BL_B0FD45910.1	Os02g0275200	449	No
TaFUT-K	Not present	Os06g0212600	501	No
TaFUT-L	Not present	Os06g0211600	513	No
TaFUT-M	Traes_5BL_9812A4B62.9	Os09g0458100	494	No
TaFUT-N	Not present	Os06g0212500	489	No
TaFUT-O	Traes_6AL_D0DAF923E.1 Traes_6BL_F1AC805AA.2 Traes_6DL_E31E7DEE8.1	Os02g0764400	555	Yes
TaFUT-P	Traes_6DL_1334C2E40.1	Os02g0763800	344	No
Not identified	Not present	Os08g0334900		

968
969

970 **Table 5:** List of primers used for expression profiling of wheat *FUT* genes by RT-PCR**.**

Gene	**Forward primer**	**Reverse primer**
TaFUT-A	5'-GAAGATCGGCTTCCAGATCA-3'	5'- TAGTAGAGGCCCCGGATCTT -3'
TaFUT-B	5'-TCTTCTGCGACGACGGACAG-3'	5'- CTCCTGCTCCTGGTGGTGGT-3'
TaFUT-C	5'-TAGCAACATCATCCGCTACG-3'	5'-AGGTACCTGCCAAGATGGTG-3'
TaFUT-D	5'-TCCCTATGCGTACCTCCATC-3'	5'-AAGAAGATACCGGCCCAAGT -3'
TaFUT-E	5'ACGAGGAGCGGCAGATAAT-3'	5'-CGAGACAGCTCCTCCTTGTT-3'
TaFUT-F	5'- ACGCGAACATGGTGAAGAA-3'	5'-GGAAGCAGACCCTCCTTCTG-3'
TaFUT-I	5'-GAAGACGCGTAGCTGGATG-3'	5'-GGCGACAAGAGGTTCTTCTG-3'
TaFUT-O	5'- ACAGGAAAGCCTGGGCAG-3'	5'- TTGGATAGGAAATACGCACCACATC-3'
Ta54227	5'- AAATACGCCATCAGGGAGAACATC-3'	5'- CGCTGCCGAAACCACGAGAC-3'

971

Figure legends

Figure 1: Electrospray ionization mass spectrometry (ESI-MS) analysis of XyG oligosaccharides (XyGOs) from root and shoots (coleoptile) walls of 6-day-old etiolated wheat seedlings. XyGOs were released from KOH-extracted polymers by treatment with purified XyG-specific endoglucanase XG5 from *Aspergillus aculeatus*. Panel A, Typical ESI-MS spectrum of XyGOs from roots. Panel B, Typical ESI-MS spectrum of XyGOs from shoots. Panel C, Typical ESI-MS spectrum of solubilized material from incubation of boiled XG5 enzyme with KOH extracts from wheat roots. Panel D, Typical ESI-MS of purified pea XyGOs used as controls. Pea XyG was digested with purified XG5 and XyGOs released were purified on Bio-gel-P2 column. * Indicates contaminant impurities from the enzyme or KOH extracts.

Figure 2: Collision-induced dissociation mass spectrometry analysis (CID-MS/MS) of XyGOs from wheat roots (see Fig. 1, Panel A). Typical CID-MS/MS spectra of ions at *m/z* 792 Hex3Pen2 (Panel A), *m/z* 953 Hex4Pen2 (Panel B), *m/z* 1085 Hex4Pen3 (Panel C), and *m/z* 1115 Hex5Pen2 (Panel D). Structures of some oligosaccharides deduced from MS/MS data are shown with fragmentation scheme on the right of each panel. Note the presence of “arabinosyl-xylose” and “galactosyl-xylose” side chains.

Figure 3: Xyloglucan-fucosyltransferase activity in Golgi-enriched microsomal membranes from wheat roots. Panel A, Wheat activity in Triton-X100-solubilized proteins from microsomal membranes obtained from roots of five-, eight-, and 11-day-old etiolated wheat seedlings. The activity is measured as the amount of [^{14}C]Fuc transfer onto tamarind XyG (expressed as cpm/reaction). Reactions lacking tamarind XyG (acceptor) are used as negative controls. Panel

995 B, Picture of five- and eight-day-old etiolated wheat seedlings given as a reference. Panel C,
996 Specificity of the wheat activity tested on several cell wall polymers as substrate acceptors (*i.e,*
997 arabinan, pectic galactan, RGI from potato, RGI from soybean) compared to tamarin XyG using
998 Triton-X100-solubilized proteins. Reactions lacking either the acceptor or the enzyme are
999 included to show that [^{14}C]Fuc incorporation is XyG-dependent. Error bars in panels A and C
1000 represent the SE of at least two biological replicates.
1001
1002 **Figure 4**. Effect of divalent ions (Panel A) and pH (Panel B) on wheat XyG-fucosyltransferase
1003 enzyme activity and analysis of its radiolabeled products by HPAEC (Panel C). XyG-
1004 fucosyltransferase activity was measured in Triton-X100-solubilized proteins from pea
1005 microsomal membranes (reaction conditions are provided in Materials and Methods).
1006 [^{14}C]fucose-tamarind XyG product was generated by incubating detergent-solubilized proteins
1007 from wheat root microsomes in the presence of GDP-[^{14}C]fucose and tamarind XyG, and then
1008 digested with endoglucanase (Megazyme). The released [^{14}C]fucosylated tamarind XyGOs were
1009 fractionated by HPAEC on a CarboPac PA200 column (Panel C). Control reactions containing
1010 no tamarind XyG (■) are compared to the assay containing tamarind XyG as substrate acceptor
1011 (●). Elution time of known fucosylated XyGOs (XXFG, XLFG) used as standards are indicated
1012 at the top of the peaks. Error bars in panel A represent the SE of at least two biological
1013 replicates.
1014
1015 **Figure 5**: Phylogenetic and expression analyses of wheat members of the GT37 family. Panel A,
1016 Phylogenetic analysis of Arabidopsis (black, At-), wheat (blue, Ta-), and rice (red, Os-)
1017 members of GT37 family. Pea FUT1 (green) is also included. The tree was constructed with

protein sequences using Phylogeny.fr platform as described in "Materials and Methods." Branch support (to infer bootstrap values) is based on an approximation of the standard Likelihood Ratio Test. Panel B, RT-PCR for nine *TaFUT* genes using cDNA prepared from total RNA from root and shoot from five-day-old etiolated wheat seedlings. The control gene, *Ta54227*, encodes for a AAA-family member of ATPases [79].

Figure 6: Expression profiles of *OsMUR2* and its closest homolog *Os06g0212100*. Expression data is obtained from eFP platform (http://bar.utoronto.ca/efprice/cgi-bin/efpWeb.cgi). Note that both genes have similar expression levels in roots and that the expression is mostly confined to roots.

Acknowledgments

The authors would like to thank Dr. Kirk Schnorr from Novozyme (Denmark) for generously providing XyG-specific endoglucanase XG5, EGII from *Aspergillus aculeatus*. We also thank Dr. Michael Hahn, Dr. Siva Pattathil, and Dr. Samuel Hazen for their precious comments on the manuscript. This work is dedicated to the memory of Prof. Gordon Maclachlan (McGill University, Montreal, Canada).

Abbreviations

ESI	Electrospray ionization
CID	Collision-induced dissociation
GC-MS	Gas chromatography mass spectrometer
Glc	Glucose
Xyl	Xylose
Gal	Galactose
Ara	Arabinose
Fuc	Fucose
XyG	Xyloglucan
XyGOs	Xyloglucan oligosaccharides
TXyG	Tamarind xyloglucan
HPAEC	High pH anion exchange chromatography
PAD	Pulsed-amperometric detection
AIR	Alcohol-insoluble residue
RT	Reverse transcription
CAZy	Carbohydrate-active enzyme

Fig. 1

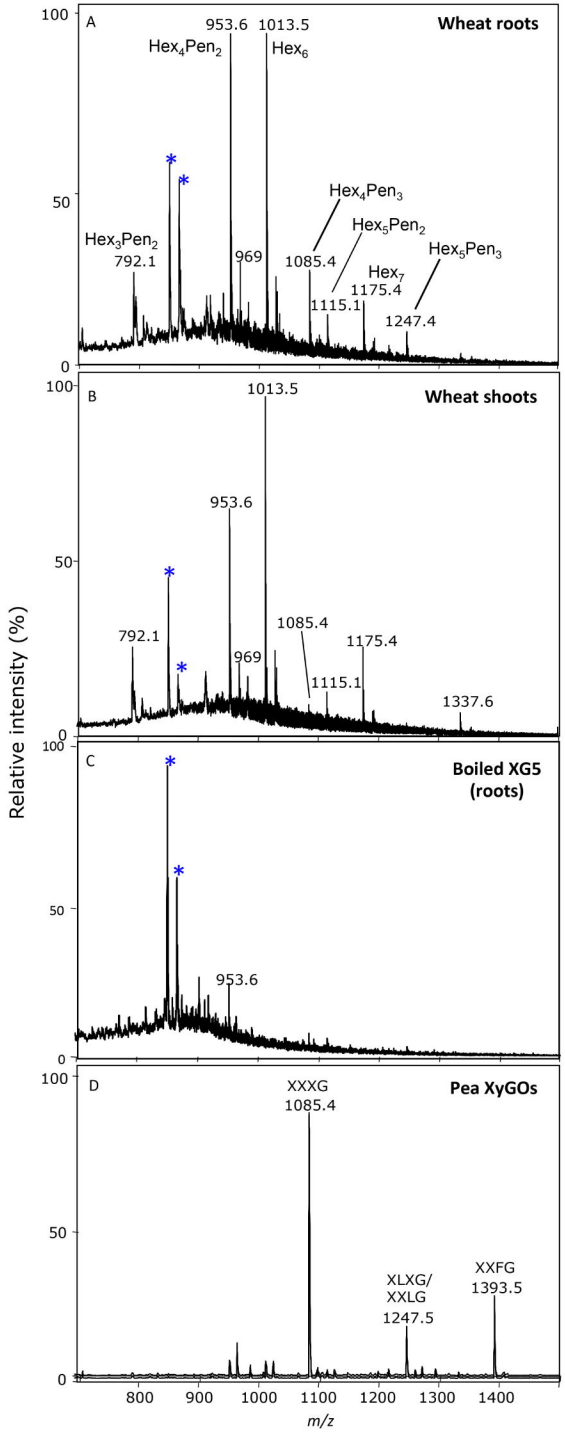
A
Wheat roots
953.6
1013.5
Hex4Pen2
Hex6
Hex4Pen3
Hex5Pen2
Hex5Pen3
Hex3Pen2
792.1
969
1085.4
Hex7
1175.4
1115.1
1247.4
B
Wheat shoots
1013.5
953.6
792.1
1085.4
969
1175.4
1115.1
1337.6
C
Boiled XG5
(roots)
953.6
D
Pea XyGOs
XXXG
1085.4
XLXG/
XXLG
1247.5
XXFG
1393.5
Relative intensity (%)
m/z
100
50
0
800
900
1000
1100
1200
1300
1400

Fig. 2

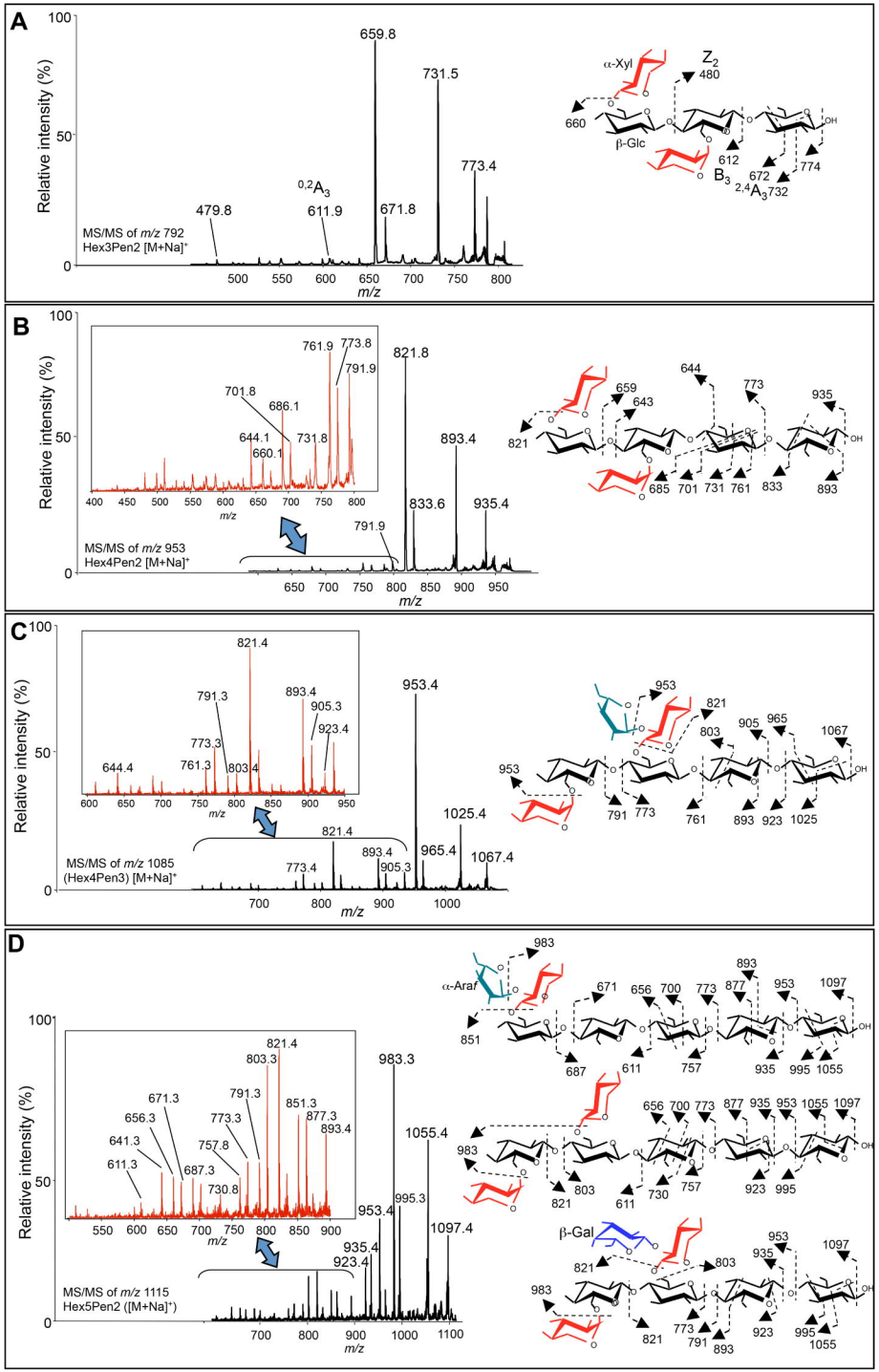
A
Relative intensity (%)
659.8
731.5
773.4
479.8
611.9
671.8
0,2A3
MS/MS of m/z 792
Hex3Pen2 [M+Na]+
m/z
α-Xyl
Z2
480
660
β-Glc
612
B3
672
2,4A3732
774
B
761.9
773.8
791.9
701.8
686.1
644.1
660.1
731.8
821.8
893.4
833.6
935.4
791.9
MS/MS of m/z 953
Hex4Pen2 [M+Na]+
644
659
643
773
935
821
685
701
731
761
833
893
C
821.4
791.3
893.4
905.3
923.4
773.3
644.4
761.3
803.4
953.4
1025.4
821.4
893.4
965.4
1067.4
773.4
905.3
MS/MS of m/z 1085
(Hex4Pen3) [M+Na]+
953
821
905
965
1067
803
791
773
761
893
923
1025
D
821.4
803.3
983.3
671.3
791.3
851.3
656.3
773.3
877.3
893.4
641.3
757.8
1055.4
611.3
687.3
730.8
995.3
953.4
1097.4
935.4
923.4
MS/MS of m/z 1115
Hex5Pen2 ([M+Na]+)
α-Araf
983
851
671
656
700
773
877
893
953
1097
687
611
757
935
995
1055
803
730
821
923
β-Gal

Fig. 3

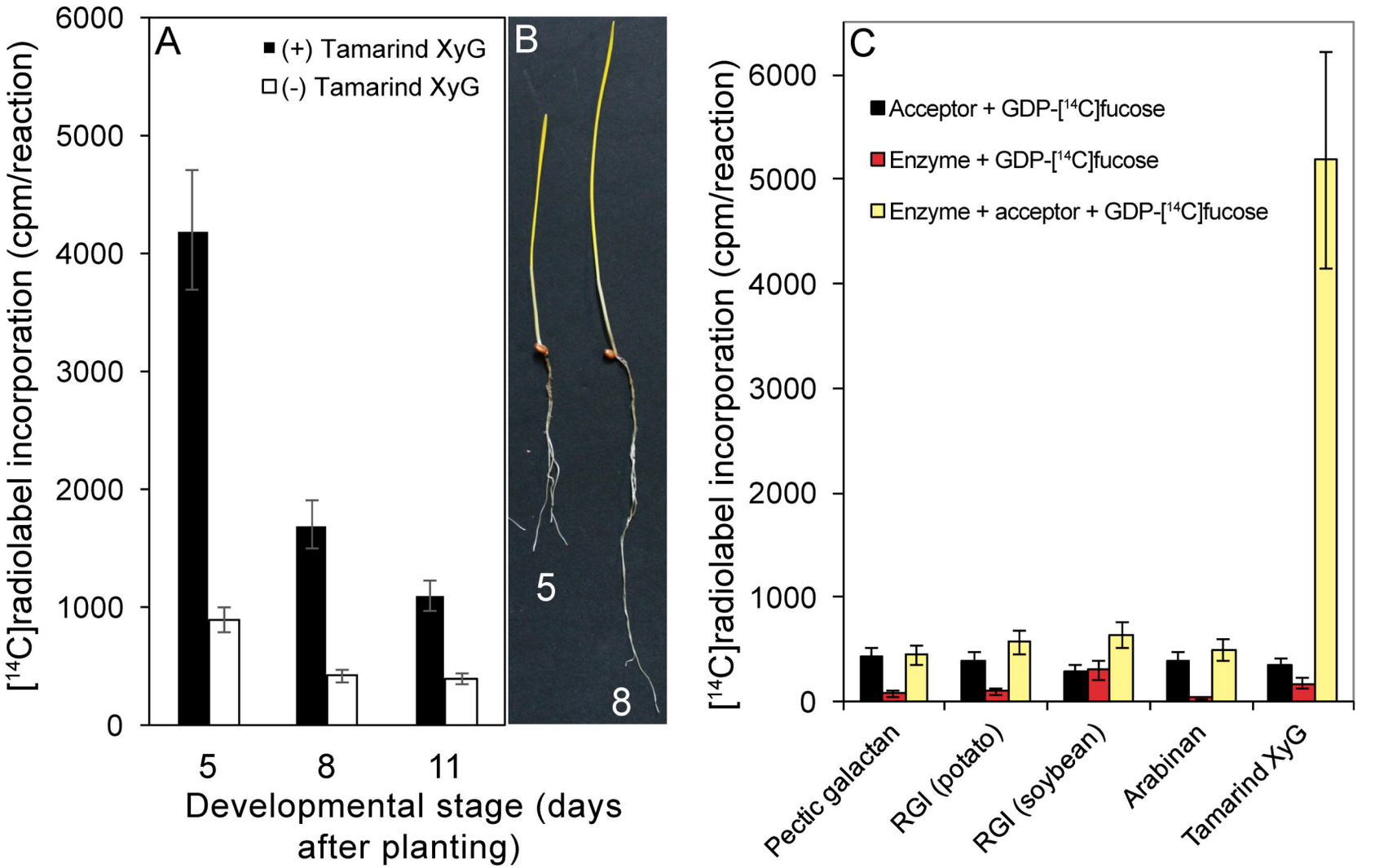
A
(+) Tamarind XyG
(-) Tamarind XyG
[14C]radiolabel incorporation (cpm/reaction)
6000
5000
4000
3000
2000
1000
0
5
8
11
Developmental stage (days after planting)
B
5
8
C
Acceptor + GDP-[14C]fucose
Enzyme + GDP-[14C]fucose
Enzyme + acceptor + GDP-[14C]fucose
[14C]radiolabel incorporation (cpm/reaction)
Pectic galactan
RGI (potato)
RGI (soybean)
Arabinan
Tamarind XyG

Fig. 4

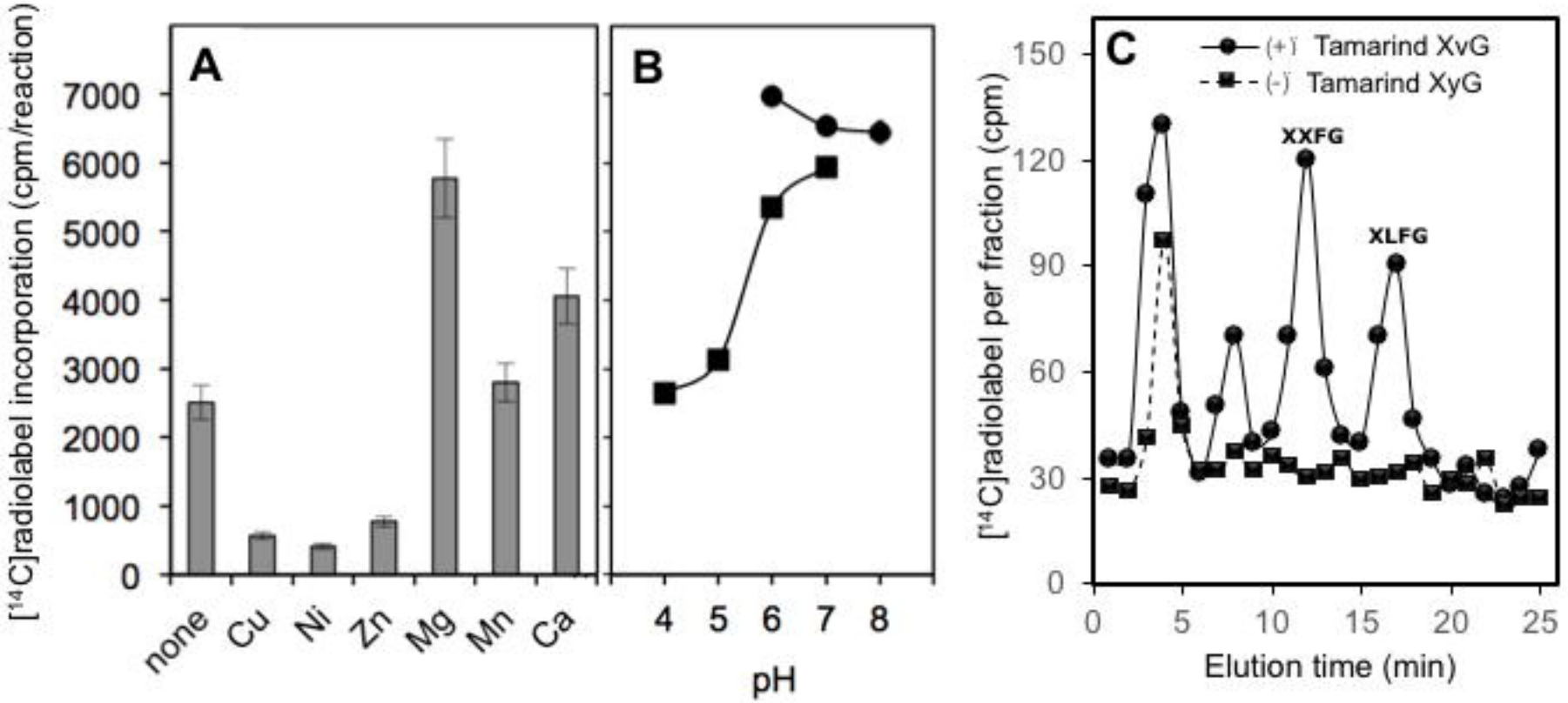
A
B
C
[14C]radiolabel incorporation (cpm/reaction)
7000
6000
5000
4000
3000
2000
1000
0
none
Cu
Ni
Zn
Mg
Mn
Ca
4
5
6
7
8
pH
[14C]radiolabel per fraction (cpm)
150
120
90
60
30
0
(+) Tamarind XvG
(-) Tamarind XyG
XXFG
XLFG
0
5
10
15
20
25
Elution time (min)

Fig. 5

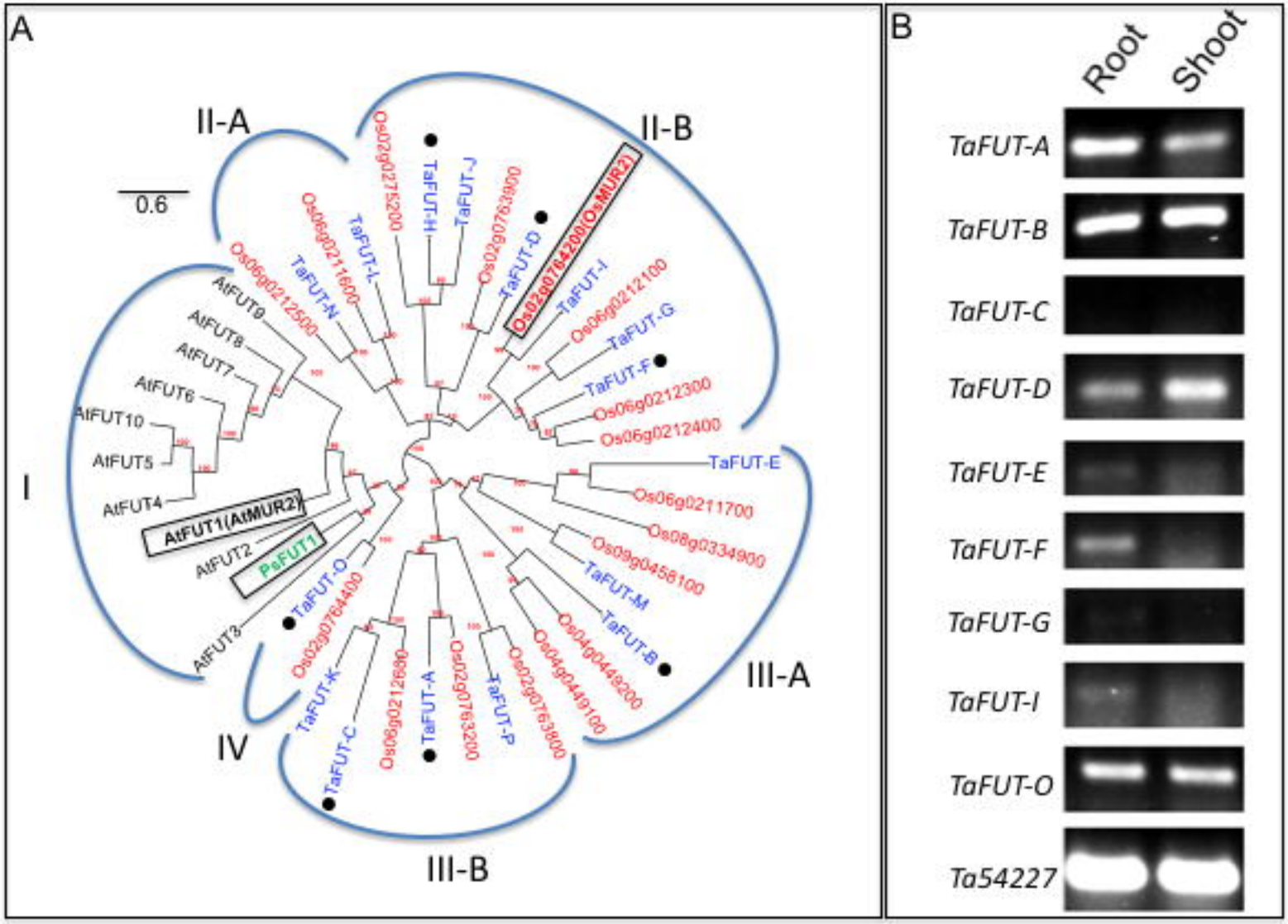
A
II-A
II-B
0.6
I
III-A
IV
III-B
AtFUT9
AtFUT8
AtFUT7
AtFUT6
AtFUT10
AtFUT5
AtFUT4
AtFUT1(AtMUR2)
AtFUT2
PeFUT1
AtFUT3
Os06g0212500
TaFUT-N
Os06g0211600
TaFUT-L
Os02g0275200
TaFUT-H
TaFUT-J
Os02g0763900
TaFUT-D
Os02g0764200(OsMUR2)
TaFUT-I
Os06g0212100
TaFUT-G
TaFUT-F
Os06g0212300
Os06g0212400
TaFUT-E
Os06g0211700
Os08g0334900
Os09g0458100
TaFUT-M
TaFUT-B
Os04g0448200
Os04g0449100
Os02g0763800
TaFUT-P
Os02g0763200
TaFUT-A
Os06g0212600
TaFUT-C
TaFUT-K
Os02g0764400
TaFUT-O
B
Root
Shoot
TaFUT-A
TaFUT-B
TaFUT-C
TaFUT-D
TaFUT-E
TaFUT-F
TaFUT-G
TaFUT-I
TaFUT-O
Ta54227

Fig. 6

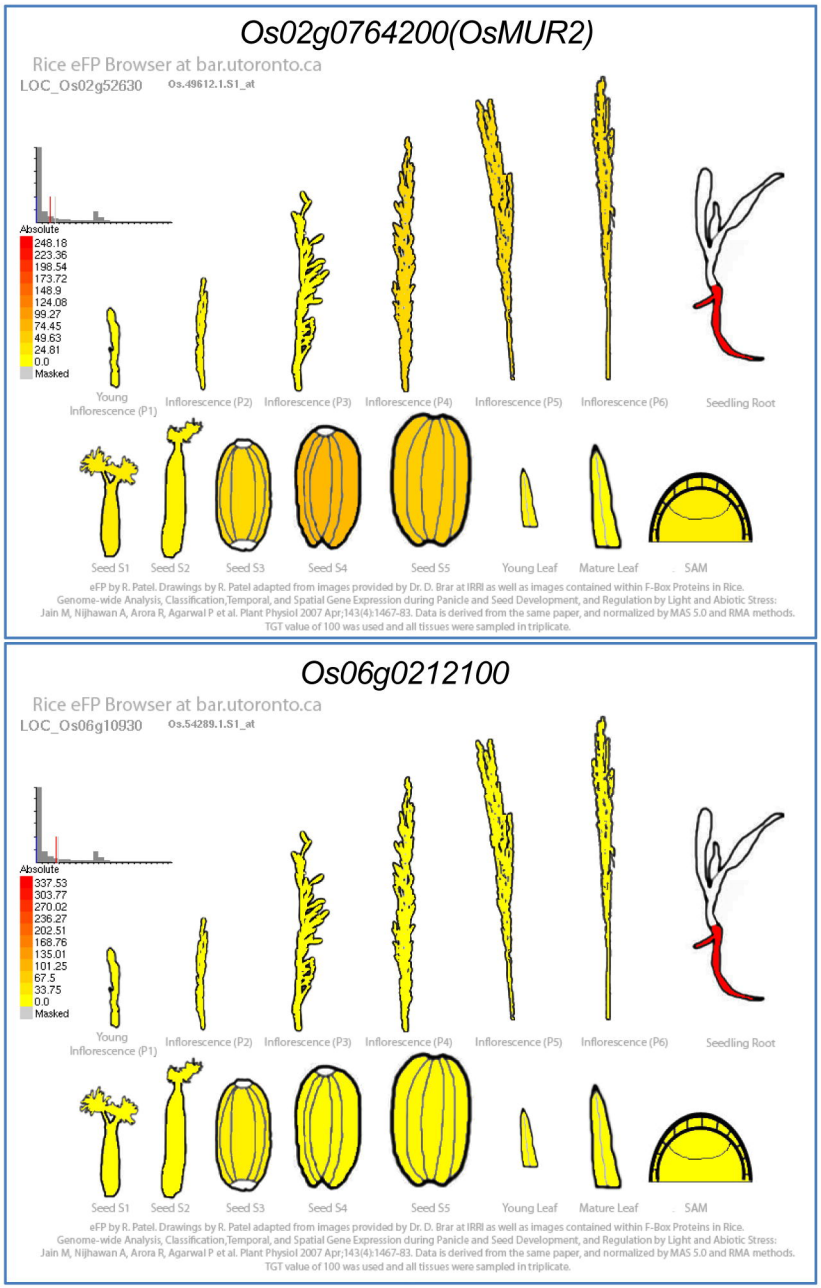
Os02g0764200(OsMUR2)
Rice eFP Browser at bar.utoronto.ca
LOC_Os02g52630
Os.49612.1.S1_at
Absolute
248.18
223.36
198.54
173.72
148.9
124.08
99.27
74.45
49.63
24.81
0.0
Masked
Young Inflorescence (P1)
Inflorescence (P2)
Inflorescence (P3)
Inflorescence (P4)
Inflorescence (P5)
Inflorescence (P6)
Seedling Root
Seed S1
Seed S2
Seed S3
Seed S4
Seed S5
Young Leaf
Mature Leaf
SAM
eFP by R. Patel. Drawings by R. Patel adapted from images provided by Dr. D. Brar at IRRI as well as images contained within F-Box Proteins in Rice.
Genome-wide Analysis, Classification,Temporal, and Spatial Gene Expression during Panicle and Seed Development, and Regulation by Light and Abiotic Stress:
Jain M, Nijhawan A, Arora R, Agarwal P et al. Plant Physiol 2007 Apr;143(4):1467-83. Data is derived from the same paper, and normalized by MAS 5.0 and RMA methods.
TGT value of 100 was used and all tissues were sampled in triplicate.
Os06g0212100
Rice eFP Browser at bar.utoronto.ca
LOC_Os06g10930
Os.54289.1.S1_at
Absolute
337.53
303.77
270.02
236.27
202.51
168.76
135.01
101.25
67.5
33.75
0.0
Masked
Young Inflorescence (P1)
Inflorescence (P2)
Inflorescence (P3)
Inflorescence (P4)
Inflorescence (P5)
Inflorescence (P6)
Seedling Root
Seed S1
Seed S2
Seed S3
Seed S4
Seed S5
Young Leaf
Mature Leaf
SAM
eFP by R. Patel. Drawings by R. Patel adapted from images provided by Dr. D. Brar at IRRI as well as images contained within F-Box Proteins in Rice.
Genome-wide Analysis, Classification,Temporal, and Spatial Gene Expression during Panicle and Seed Development, and Regulation by Light and Abiotic Stress:
Jain M, Nijhawan A, Arora R, Agarwal P et al. Plant Physiol 2007 Apr;143(4):1467-83. Data is derived from the same paper, and normalized by MAS 5.0 and RMA methods.
TGT value of 100 was used and all tissues were sampled in triplicate.